Eigenvalue density of Wilson loops in $2D$ SU(N) YM

JHEP05(2009)107

(http://iopscience.iop.org/1126-6708/2009/05/107)

Published by IOP Publishing for SISSA

Received: *May 4, 2009*
Accepted: *May 14, 2009*
Published: *May 26, 2009*

JHEP05(2009)107

Eigenvalue density of Wilson loops in $2D$ SU(N) YM

Robert Lohmayer,[a] **Herbert Neuberger**[b] **and Tilo Wettig**[a]

[a] *Institute for Theoretical Physics, University of Regensburg, 93040 Regensburg, Germany*
[b] *Department of Physics and Astronomy, Rutgers University, Piscataway, NJ 08855, U.S.A.*
E-mail: robert.lohmayer@physik.uni-regensburg.de, neuberg@physics.rutgers.edu, tilo.wettig@physik.uni-regensburg.de

Abstract: In 1981 Durhuus and Olesen (DO) showed that at infinite N the eigenvalue density of a Wilson loop matrix W associated with a simple loop in two-dimensional Euclidean SU(N) Yang-Mills theory undergoes a phase transition at a critical size. The averages of $\det(z-W)$, $\det(z-W)^{-1}$, and $\det(1+uW)/(1-vW)$ at finite N lead to three different smoothed out expressions, all tending to the DO singular result at infinite N. These smooth extensions are obtained and compared to each other.

Keywords: Matrix Models, Lattice Gauge Field Theories, 1/N Expansion

ArXiv ePrint: 0904.4116

doi:10.1088/1126-6708/2009/05/107

Contents

JHEP05(2009)107

1 Introduction

So far, the large-N limit of SU(N) YM theory has been mainly employed for qualitative insights. Our objective is to find a way to exploit the simplifications at large N for actual first-principles quantitative calculations of at least some nonperturbative quantities in theories that interact weakly at short distances and strongly at long distances. To be sure, significantly more work is needed in order to construct a real calculational framework; we are not there yet.

In two Euclidean dimensions the eigenvalue distribution of the SU(N) Wilson matrix associated with a non-selfintersecting loop undergoes a phase transition in the infinite-N limit as the loop is dilated [1]. This phase transition has universal properties shared across dimensions and across analog two-dimensional models [2, 3]. Thus, a detailed understanding of the transition region in 2D is of relevance to crossovers from weakly to strongly interacting regimes in a wide class of models based on doubly-indexed dynamical variables with symmetry SU(N). Building upon previous work [4–6], this paper presents several new results in this context and indicates how such results might be used to estimate long-distance parameters by analytical means, at least for $N \gg 1$.

We are focusing on the eigenvalues of the Wilson loop. The associated observables are three different functions $\rho_N^\ell(\theta)$, with ℓ = asym, sym, true, of an angular variable θ. At infinite N the three functions have identical limits: $\rho_\infty^\ell(\theta) = \rho_\infty(\theta)$. For a specific critical scale, the nonnegative function $\rho_\infty(\theta)$ exhibits a transition at which a gap centered at $\theta = \pm\pi$, present for small loops, just closes. This transition was discovered by Durhuus and Olesen in 1981 [1].

For the time being, we shall suppress the size dependence of the $\rho_N^\ell(\theta)$. $\rho_N^\ell(\theta)$ for ℓ = asym, sym are obtained from the logarithmic derivative of $\langle \det^k(z-W)\rangle$ for $k = 1$ and -1, respectively. One needs to take z to $e^{i\theta}$ in a specified manner. Neither of these two functions $\rho_N^\ell(\theta)$ has a natural interpretation at finite N; the interest in these functions mainly stems from them obeying simple partial integro/differential equations which are exactly integrable and already known and studied in other contexts [4, 5]. In the course of this paper we extend the results in [4, 5].

Unlike $\rho_N^\ell(\theta)$ with ℓ = asym, sym, $\rho_N^{\rm true}(\theta)$ literally is the eigenvalue density at finite N, $\langle {\rm Tr}\,\delta(\theta + i\log W)\rangle$, and poses no difficulties of interpretation. It can be obtained from $\langle \det(1+uW)/(1-vW)\rangle$ in the limit $-u \to v \to e^{i\theta}$. We shall derive expressions for $\rho_N^{\rm true}(\theta)$ in this work. As anticipated in [5], we find no evidence that $\rho_N^{\rm true}(\theta)$ obeys as simple equations as the $\rho_N^\ell(\theta)$ for $\ell \neq$ true were found to do.

JHEP05(2009)107

This paper starts with a general description of $\rho_N^\ell(\theta)$. We then follow with details for each case. First, we describe the case $\ell = \text{asym}$, where the focus is on the loop-size dependence of the zeros z_j of the average characteristic polynomial. The equations governing these zeros were derived in [4], and here we work out the approximate solution for small, intermediate, and large loops. Then comes a description of the case $\ell = \text{sym}$ and a saddle-point analysis of the integral representation found in [5]. A connection to the multiplicative random matrix model of [7, 8] is pointed out. We then proceed to deriving exact representations of $\rho_N^{\text{true}}(\theta)$. As anticipated, we do not find a simple direct equation for $\rho_N^{\text{true}}(\theta)$, but we do find a simple equation for $\langle \det(1+uW)/(1-vW)\rangle$. From this we obtain a representation of $\rho_N^{\text{true}}(\theta)$ by a sum. By numerically performing the sum, $\rho_N^{\text{true}}(\theta)$ can be evaluated to any desired accuracy. Further, we obtain an integral representation for $\rho_N^{\text{true}}(\theta)$ which is useful for setting up the $1/N$ expansion of $\rho_N^{\text{true}}(\theta)$. We carry out the saddle-point analysis which is the starting point of this expansion. We also show that one can define a natural extension to negative values of N, and in this extension $\rho_N^{\text{true}}(\theta) = \rho_{-N}^{\text{true}}(\theta)$. We follow this by a numerically aided study of the relations between the three $\rho_N^\ell(\theta)$. We compare numerically the densities $\rho_N^{\text{true}}(\theta)$ and $\rho_N^{\text{sym}}(\theta)$ at the same areas. As $\rho_N^{\text{asym}}(\theta)$ is given by a sum of δ-functions, its comparison to another $\rho_N^\ell(\theta)$ is less direct. We conjecture, and check numerically, that the location of the N peaks in $\rho_N^{\text{true}}(\theta)$ are close to the matching zeros $\theta_j = -i\log z_j$ of the average characteristic polynomial. By "close" we mean that for large N the distance between a θ_j and the matching peak vanishes faster than the distance between that peak and its adjacent valley.

In order to indicate how this paper fits into a larger research plan, we finish with a sketch of the bigger motivating picture.

2 Three "densities" $\rho_N^\ell(\theta)$ and how they compare

2.1 Different definitions of dimensionless area

The dimensionless area variable has to take a slightly different form for the average of the characteristic polynomial and the average of its inverse to obey equations that look simple.

We define

$$t = \mathcal{A}g^2N\,, \tag{2.1}$$

where $\mathcal{A}$ is the area enclosed by the Wilson loop, g is the YM coupling, and the gauge group is SU(N). $\lambda = g^2N$ is the standard 't Hooft coupling, and t makes it dimensionless. This t appears in $\rho_N^{\text{true}}(\theta, t)$.

The average characteristic polynomial generates the expectation values of the characters of all antisymmetric representations of the Wilson loop matrix. The appropriate area variable in this case is denoted by τ, with [5]

$$\tau = t\left(1+\frac{1}{N}\right)\,. \tag{2.2}$$

Thus, when $\rho_N^{\text{asym}}(\theta,\tau)$ is compared to $\rho_N^{\text{true}}(\theta,t)$, the $1/N$ correction in t relative to τ has to be taken into account.

JHEP05(2009)107

The average of the inverse of the characteristic polynomial generates the expectation values of the characters of all symmetric representations of the Wilson loop matrix. The appropriate area variable in this case is denoted by T, with [5]

$$T = t\left(1 - \frac{1}{N}\right) . \tag{2.3}$$

Thus, when $\rho_N^{\rm sym}(\theta, T)$ is compared to $\rho_N^{\rm true}(\theta, t)$, the $1/N$ correction in t relative to T has to be taken into account.

2.2 Averaging over the SU(N) Wilson loop matrix W

The probability density for W is given by the heat kernel (see for example [9] and original references therein)

$$\mathcal{P}_N(W, t) = \sum_r d_r \chi_r(W) e^{-\frac{t}{2N} C_2(r)} \tag{2.4}$$

with $t = \lambda \mathcal{A}$, where the sum over r is over all distinct irreducible representations of SU(N) with d_r denoting the dimension of r and $C_2(r)$ denoting the value of the quadratic Casimir on r. $\chi_r(W)$ is the character of W in the representation r and is normalized by $\chi_r(\mathbf{1}) = d_r$. Averages over W at fixed t are given by

$$\langle \mathcal{O}(W) \rangle = \int dW \mathcal{P}_N(W, t) \mathcal{O}(W) , \tag{2.5}$$

where dW is the Haar measure on SU(N) normalized by $\int dW = 1$. Note that we have $\int dW \mathcal{P}_N(W, t) = 1$. Any class function can be averaged when expanded in characters using character orthogonality.

Because in the sum over r in (2.4) each representation is accompanied by its complex conjugate representation, it is easy to see that

$$\langle \mathcal{O}(W) \rangle = \langle \mathcal{O}(W^\dagger) \rangle = \langle \mathcal{O}(W^*) \rangle , \tag{2.6}$$

implying identities relating $\langle \det(z - W) \rangle$, $\langle \det(z - W)^{-1} \rangle$, and $\langle \det(1 + uW)/(1 - vW) \rangle$ to the same objects with $z \to 1/z$, $z \to z^*$, $u, v \to 1/u, 1/v$, and $u, v \to u^*, v^*$, respectively.

2.3 General features of the $\rho_N^\ell(\theta)$

The ρ_N^ℓ are real on the unit circle parametrized by the angle $|\theta| \leq \pi$, even under $\theta \to -\theta$, and depend on the size of the loop. All three are positive distributions in θ, normalized by

$$\int_{-\pi}^{\pi} \frac{d\theta}{2\pi} \rho_N^\ell(\theta) = 1 . \tag{2.7}$$

$\rho_N^{\rm asym}$ summarizes the averages of the characters of W in all totally antisymmetric representations, i.e., single-column Young diagrams. $\rho_N^{\rm sym}$ summarizes the averages of the characters of W in all totally symmetric representations, i.e., single-row Young diagrams. $\rho_N^{\rm true}$ summarizes the averages of the traces of all k-wound Wilson loops matrices, $\langle \mathrm{Tr}\, W^k \rangle$.

JHEP05(2009)107

As we will discuss in section 5, the latter are determined by linear combinations of the averages of the characters of W in representations which we label by (p, q) and whose Young diagrams have the following shape:

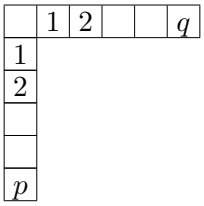

(2.8)

$\rho_N^{\rm true}$ determines $\langle \mathrm{Tr}\, f(W)\rangle$ for any function f. However, unlike $\rho_N^{\rm asym}$ and $\rho_N^{\rm sym}$, it has no information about any average of the type $\langle \mathrm{Tr}\, f(W)\, \mathrm{Tr}\, g(W)\rangle$, where the number of trace factors exceeds one. In other words, $\rho_N^{\rm true}$ is the single eigenvalue density and, unlike $\rho_N^{\rm asym}$ and $\rho_N^{\rm sym}$, contains no information about any higher-point eigenvalue correlations.

2.4 $\rho_N^{\mathbf{asym}}(\theta,\tau)$

$\rho_N^{\rm asym}(\theta,\tau)$ is constructed from the logarithmic derivative of the average of the characteristic polynomial, whose zeros are $z_j(\tau) = \exp(i\theta_j(\tau))$ with $j = 0, \ldots, N-1$ and $-\pi \le \theta_j \le \pi$,

$$\psi^{(N)}(z,\tau) \equiv \langle \det(z - W)\rangle = \prod_{j=0}^{N-1} (z - z_j(\tau))\,. \tag{2.9}$$

Define

$$\phi^{(N)}(z,\tau) = \frac{i}{N}\frac{1}{\psi^{(N)}(z,\tau)}\left[z\frac{\partial}{\partial z} + \frac{N}{2}\right]\psi^{(N)}(z,\tau)\,. \tag{2.10}$$

Setting $z = e^{-iy}$ we obtain

$$\phi^{(N)}(e^{-iy},\tau) = i - \frac{1}{N}\sum_{j=0}^{N-1}\sum_{n\in\mathbb{Z}}\frac{1}{y + \theta_j + 2\pi n}\,. \tag{2.11}$$

We set y to $\theta \pm i\epsilon$ with $\epsilon > 0$ and real θ and define

$$\varphi_\pm^{(N)}(\theta,\tau) = \lim_{\epsilon\to 0}\phi^{(N)}(e^{-i(\theta\pm i\epsilon)},\tau)\,. \tag{2.12}$$

Finally, we define $\rho_N^{\rm asym}(\theta,\tau)$ in analogy to $\rho_N^{\rm sym}(\theta,T)$ in [5],

$$\begin{aligned}\rho_N^{\rm asym}(\theta,\tau) &= -2\,\mathrm{Re}\left[i\varphi_+^{(N)}(\theta,\tau) + 1\right] = -i\left[\varphi_+^{(N)}(\theta,\tau) - \varphi_-^{(N)}(\theta,\tau)\right]\\ &= \frac{2\pi}{N}\sum_{j=0}^{N-1}\delta_{2\pi}\left(\theta + \theta_j(\tau)\right) = \frac{2\pi}{N}\sum_{j=0}^{N-1}\delta_{2\pi}\left(\theta - \theta_j(\tau)\right)\,,\end{aligned} \tag{2.13}$$

where $\delta_{2\pi}$ denotes the 2π-periodized δ-function with normalization

$$\int_{-\pi}^{\pi} d\theta\, \delta_{2\pi}(\theta) = 1 \tag{2.14}$$

JHEP05(2009)107

and the last identity in (2.13) follows from the fact that $\rho_N^{\rm asym}(\theta,\tau)$ is even in θ. The sum over δ-functions will reproduce exactly the averages of the traces of W in all totally antisymmetric representations at arbitrary finite N, simply by setting W equal to $\mathrm{diag}(e^{i\theta_0(\tau)}, e^{i\theta_1(\tau)}, \ldots, e^{i\theta_{N-1}(\tau)})$. Thus, the entire information of $\rho_N^{\rm asym}(\theta,\tau)$ is contained in the set $\theta_j(\tau)$. It is obvious that given $\rho_N^{\rm asym}(\theta,\tau)$ we can reconstruct $\phi^{(N)}(z,\tau)$ and $\psi^{(N)}(z,\tau)$. The infinite-N limit of $\rho_N^{\rm asym}(\theta,\tau)$ is $\rho_\infty(\theta,\tau)$ [2].

In [4] it was shown that the $\theta_j(\tau)$ are determined by a set of first-order "equations of motion" in τ with a specific initial condition,

$$\dot\theta_j \equiv \frac{\partial\theta_j}{\partial\tau} = \frac{1}{2N}\sum_{k\neq j}\cot\frac{\theta_j-\theta_k}{2}\,. \tag{2.15}$$

The initial condition

$$\theta_j(0) = 0 \tag{2.16}$$

is at a singular point of the differential equations. However, once one understands that as τ grows from zero the $\theta_j(\tau)$ spread out, the solution becomes uniquely determined. Throughout the evolution, the $\dot\theta_j$ never change sign. For any $\tau > 0$ we have

$$\theta_0(\tau) < \theta_1(\tau) < \ldots < \theta_{N-1}(\tau)\,. \tag{2.17}$$

There is a $\mathbb{Z}_2$ symmetry pairing them,

$$\theta_{N-j-1}(\tau) = -\theta_j(\tau)\,. \tag{2.18}$$

If N is odd (2.18) yields

$$\theta_{\frac{N-1}{2}}(\tau) = 0\,. \tag{2.19}$$

Thus, there are $[N/2]$ pairs of nonzero eigenvalues of opposite signs, implying $\rho_N^{\rm asym}(\theta,\tau) = \rho_N^{\rm asym}(-\theta,\tau)$.

In section 3 we shall calculate the behavior of the $\theta_j(\tau)$ at small, critical, and large τ.

2.5 $\rho_N^{\rm sym}(\theta,T)$

$\rho_N^{\rm sym}(\theta,T)$ is constructed from the logarithmic derivative of the average of the inverse characteristic polynomial. We reproduce here the relevant formulas from [5]. Define

$$\psi_\pm^{(N)}(z,T) = \langle \det(z-W)^{-1}\rangle\,, \tag{2.20}$$

where $+$ is for $|z|>1$ and $-$ for $|z|<1$. Because of the negative power, one cannot exclude singularities at $|z|=1$ (although equation (22) of [5] shows that these singularities are removable so that $\psi_\pm^{(N)}(z,T)$ can be continued to $|z|=1$). One should think about $\psi_\pm^{(N)}(z,T)$ as two distinct functions. They are simply related to each other by

$$\psi_-^{(N)}(1/z,T) = (-z)^N\psi_+^{(N)}(z,T)\,, \qquad |z|>1\,. \tag{2.21}$$

We now define

$$\phi_\pm^{(N)}(z,T) = \frac{i}{N}\frac{1}{\psi_\pm^{(N)}(z,T)}\left(z\frac{\partial}{\partial z}+\frac{N}{2}\right)\psi_\pm^{(N)}(z,T)\,. \tag{2.22}$$

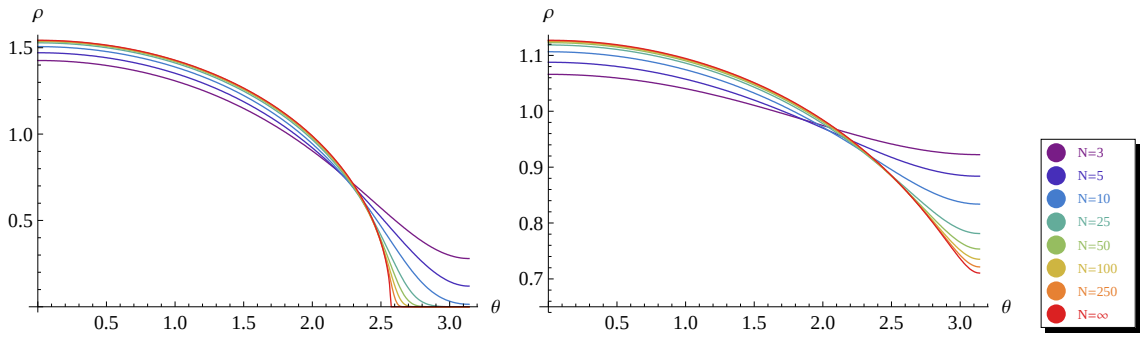

Figure 1. Plots of $\rho_N^{\rm sym}(\theta,T)$ for $T=2$ (left), $T=5$ (right), and $N=3,5,10,25,50,100,250$ together with $\rho_\infty(\theta,T)$.

$\rho_N^{\rm sym}(\theta,T)$ is given by

$$\rho_N^{\rm sym}(\theta,T)=i\lim_{\epsilon\to 0}\left[\phi_+^{(N)}(e^{-i\theta+\epsilon},T)-\phi_-^{(N)}(e^{-i\theta-\epsilon},T)\right]. \tag{2.23}$$

Unlike $\rho_N^{\rm asym}(\theta,\tau)$, $\rho_N^{\rm sym}(\theta,T)$ is a smooth function of θ for any finite N and $T>0$. It again obeys $\rho_N^{\rm sym}(\theta,T)=\rho_N^{\rm sym}(-\theta,T)$. The function is monotonic on each of the segments $(-\pi,0)$ and $(0,\pi)$ with the maximum at $\theta=0$ and the minimum at $\theta=\pm\pi$. The infinite-N critical point is at $T=4$. For $T>4$, $\rho_N^{\rm sym}(\theta,T)$ approaches $\rho_\infty(\theta,T)$ by power corrections in $1/N$ [5]. For $T<4$, $\rho_\infty(\theta,T)$ is zero for $|\theta|>\theta_c(T)$, where $0<\theta_c(T)<\pi$ and $\theta_c(4)=\pi$. In this interval $\rho_N^{\rm sym}(\theta,T)$ approaches zero by corrections that are exponentially suppressed in N. $\rho_N^{\rm sym}(\theta,T)$ has an explicit form in terms of rapidly converging infinite sums,

$$\rho_N^{\rm sym}(\theta,T)=1+\frac{p(\theta,T)+p^*(\theta,T)}{N}, \tag{2.24}$$

$$p(\theta,T)=\frac{\sum_{k=1}^\infty k\binom{N+k-1}{N-1}e^{ik\theta}e^{-T\frac{k(k+N)}{2N}}}{1+\sum_{k=1}^\infty\binom{N+k-1}{N-1}e^{ik\theta}e^{-T\frac{k(k+N)}{2N}}}. \tag{2.25}$$

Given $\rho_N^{\rm sym}(\theta,T)$ with $T>0$ we can reconstruct $\phi_\pm^{(N)}(z,T)$ and $\psi_\pm^{(N)}(z,T)$ using the Poisson integral, on account of the analyticity of $\psi_-^{(N)}(z,T)$ for $|z|<1$.

In [5] it was also shown that $\psi_+^{(N)}(z,T)$ for $|z|>1$ has an integral representation given by

$$\psi_+^{(N)}(z,T)=e^{\frac{NT}{8}}\sqrt{\frac{N}{2\pi T}}\int_{-\infty}^{\infty}du\,e^{-\frac{N}{2T}u^2}\left(ze^{-i\frac{u}{2}}-e^{i\frac{u}{2}}\right)^{-N}. \tag{2.26}$$

It was pointed out there that this formula exhibited a formal relation to $\langle\det(z-W)\rangle$ under a sign switch of N. Similar observations have been made in the past, see [10] and references therein.

Equation (2.25) can be evaluated numerically for arbitrary N to any desired precision. In figure 1 we show how $\rho_N^{\rm sym}(\theta,T)$ approaches the infinite-N result $\rho_\infty(\theta)$ of DO [1] for fixed $T=2$ and $T=5$. In addition to these numerical results, it would be useful to compute analytically the asymptotic expansion of $\rho_N^{\rm sym}(\theta,T)$ in $1/N$. For this it is enough to expand $\psi_+^{(N)}(z,T)$ in $1/N$, which is best done by starting from (2.26). The $1/N$ expansion then

JHEP05(2009)107

comes from an expansion around a single saddle point. This problem will be considered in section 4. The saddle points turn out to be related to the position of the boundary of the eigenvalue domain of the random multiplicative complex matrix ensemble studied in [7, 8].

In section 6 we will show plots comparing $\rho_N^{\rm sym}(\theta,T)$ to $\rho_N^{\rm true}(\theta,t)$.

2.6 $\rho_N^{\rm true}(\theta,t)$

Finally, unlike ρ_N^ℓ with $\ell = {\rm asym}, {\rm sym}$, $\rho_N^{\rm true}(\theta,t)$ has a natural definition. If the eigenvalues of W are $e^{i\alpha_j}$ with $j = 0, 1, \ldots, N-1$, we define

$$\rho_N^{\rm true}(\theta,t) = \frac{2\pi}{N}\sum_j \langle \delta_{2\pi}(\theta - \alpha_j(W))\rangle = \frac{2\pi}{N}\langle {\rm Tr}\, \delta_{2\pi}(\theta + i\log(W))\rangle\,. \tag{2.27}$$

With the help of $\rho_N^{\rm true}(\theta,t)$ we can compute the averages of a specific subset of class functions $F(W)$, namely, those that can be written as

$$F(W) = \frac{1}{N}\sum_j f(\alpha_j(W))\,. \tag{2.28}$$

The obvious formula is

$$\langle F(W)\rangle = \Big\langle \frac{1}{N}\sum_j \int_{-\pi}^{\pi} d\theta f(\theta)\delta_{2\pi}(\theta - \alpha_j(W))\Big\rangle = \int_{-\pi}^{\pi}\frac{d\theta}{2\pi} f(\theta)\rho_N^{\rm true}(\theta,t)\,. \tag{2.29}$$

$\rho_N^{\rm true}(\theta,t)$ summarizes all the information contained in the entire collection of averages of the type $\langle {\rm Tr}\, f(W)\rangle$. Viewed in this way, it is analogous to $\rho^{\rm asym}(\theta,\tau)$ and $\rho^{\rm sym}(\theta,T)$, which summarize all the information contained in all averages $\langle \chi_r(W)\rangle$, with r denoting all totally antisymmetric and all totally symmetric representations, respectively. The analog of the functions $\phi^{(N)}(z,\tau)$ and $\phi_\pm^{(N)}(z,T)$ related to $\rho^{\rm asym}(\theta,\tau)$ and $\rho^{\rm sym}(\theta,T)$, respectively, in the present case is the average resolvent,

$$\Phi_\pm^{(N)}(z,t) = \frac{1}{N}\left\langle {\rm Tr}\,\frac{1}{z-W}\right\rangle\,. \tag{2.30}$$

Here again the $+$ sign goes with $|z|>1$ and the $-$ sign goes with $|z|<1$.

Using (2.6) one easily concludes that $\Phi_+^{(N)}(z,t)$ determines $\Phi_-^{(N)}(z,t)$ just as in the case of $\phi_\pm^{(N)}(z,T)$. Clearly, $\rho_N^{\rm true}(\theta,t)$ determines $\Phi_\pm^{(N)}(z,t)$ since the latter is the average of a single trace. It is easy to see that the opposite is true also, namely, $\Phi_\pm^{(N)}(z,t)$ determines $\rho_N^{\rm true}(\theta,t)$. If we use the restrictions following from (2.6), it is enough to use just $\Phi_+^{(N)}(z,t)$ for example,

$$\rho_N^{\rm true}(\theta,t) = 2\lim_{\epsilon\to 0^+} {\rm Re}\left[e^{i\theta+\epsilon}\Phi_+^{(N)}(e^{i\theta+\epsilon},t)\right] - 1\,. \tag{2.31}$$

$\rho_N^{\rm true}(\theta,t)$ is smooth over the circle and similar to $\rho_N^{\rm sym}(\theta,T)$ in this sense, but has N peaks adding an oscillatory modulation to the function. In some sense $\rho_N^{\rm true}(\theta,t)$ is intermediate between $\rho_N^{\rm asym}(\theta,t)$ and $\rho_N^{\rm sym}(\theta,t)$, since it can be obtained from the expectation value of the ratio of values of the characteristic polynomial evaluated at two different values of its argument. The oscillatory behavior is in this sense a remnant of the δ-function structure

JHEP05(2009)107

of $\rho_N^{\text{asym}}(\theta,t)$. For this reason we expect the peaks of $\rho_N^{\text{true}}(\theta,t)$ to occur at locations close to the matching $\theta_j(\tau)$. This expectation will be confirmed numerically in section 6.

Unlike for $\ell = \text{asym}, \text{sym}$, explicit formulas for $\rho_N^{\text{true}}(\theta,t)$ were unavailable so far. New formulas that apply in this case will be derived in relative detail in section 5. We shall see that again a symmetry under $N \to -N$ exists.

3 Motion of the zeros $z_j(\tau)$ as a function of τ

In this section we only consider $\rho_N^{\text{asym}}(\theta,\tau)$ and study the zeros $z_j(\tau) = \exp(i\theta_j(\tau))$ of the average characteristic polynomial for small, large, and near the critical τ.

3.1 $\theta_j(\tau)$ for small τ

3.1.1 Approximate "equations of motion"

From equation (2.15) we obtain

$$\dot{\theta}_j = \frac{1}{N}\sum_{k\neq j}\sum_{n\in\mathbb{Z}}\frac{1}{\theta_j-\theta_k+2\pi n}\,. \tag{3.1}$$

Rescaling

$$\theta_j = \frac{\eta_j}{\sqrt{N}} \tag{3.2}$$

yields

$$\dot{\eta}_j = \sum_{k\neq j}\sum_{n\in\mathbb{Z}}\frac{1}{\eta_j-\eta_k+2\pi n\sqrt{N}}\,. \tag{3.3}$$

The initial condition $\theta_j(\tau=0)=0$ indicates that one can neglect to leading order in τ the terms with $n\neq 0$,

$$\dot{\eta}_j \approx \sum_{k\neq j}\frac{1}{\eta_j-\eta_k}\,. \tag{3.4}$$

In this approximation periodicity under $\theta_j \to \theta_j + 2\pi$ is lost, making the approximation unreliable when periodicity becomes relevant. This weak-coupling feature is a recurrent theme in models that have compact variables and become disordered at strong couplings.

3.1.2 Solution of the approximate equations

Assigning dimension 1 to τ we see that η has dimension 1/2. We define

$$\eta_j = \hat{\eta}_j\sqrt{2\tau}\,, \tag{3.5}$$

making the $\hat{\eta}_j$ variables dimensionless and therefore independent of τ. They are determined by the equations

$$\hat{\eta}_j = \sum_{k\neq j}\frac{1}{\hat{\eta}_j-\hat{\eta}_k}\,. \tag{3.6}$$

The solution of these equations is well known, see, e.g., [11, appendix A.6]. The $\hat{\eta}_j$ are the distinct zeros of the Hermite polynomial $H_N(x)$,

$$H_N(\hat{\eta}_j) = 0\,, \qquad j = 0,\ldots,N-1\,. \tag{3.7}$$

JHEP05(2009)107

3.1.3 Relation to harmonic oscillator

In the theory of orthogonal polynomials, the zeros of orthogonal polynomials are shown to be the eigenvalues of the Jacobi matrix, which is the appropriately truncated matrix of recurrence coefficients [12, Sections 2.4 and 2.11]. Introduce the matrix a_N, an N-truncated version of the infinite dimensional annihilation operator a normalized by

$$[a, a^\dagger] = 1\,. \tag{3.8}$$

The truncation is to the space spanned by the harmonic oscillator states $(a^\dagger)^j|0\rangle$ with $j = 0, \ldots, N-1$,

$$a_N = \begin{pmatrix} 0 & \sqrt{1} & 0 & 0 & \cdots & 0 & 0 \\ 0 & 0 & \sqrt{2} & 0 & \cdots & 0 & 0 \\ \vdots & \vdots & \vdots & \vdots & \vdots & \vdots & 0 \\ 0 & 0 & 0 & 0 & \cdots & 0 & \sqrt{N-1} \\ 0 & 0 & 0 & 0 & \cdots & 0 & 0 \end{pmatrix}. \tag{3.9}$$

The a_N satisfy

$$[a_N, a_N^\dagger] = \mathbf{1}_N - N P_{N-1}\,, \tag{3.10}$$

where $P_n = |n\rangle\langle n|$.

Using the recurrence relations of the Hermite polynomials, the Jacobi matrix is found to be $(a_N + a_N^\dagger)/\sqrt{2}$. Thus, to leading order in τ the zeros of $\langle \det(z - W)\rangle$ are the same as the zeros of

$$\det\left[z - e^{i\sqrt{\frac{\tau}{N}}(a_N + a_N^\dagger)}\right]. \tag{3.11}$$

3.1.4 Largest zeros

Of particular interest are the largest zeros in absolute magnitude. They come in a pair of opposite signs. Using a known formula for large N [13, eq. (6.32.5)], we have

$$\hat{\eta}_M = \sqrt{2N} - \frac{1.856}{(2N)^{1/6}} + \ldots \tag{3.12}$$

giving the largest θ_j as

$$\theta_M(\tau) = 2\sqrt{\tau}\left(1 - \frac{1.856}{(2N)^{2/3}} + \ldots\right), \qquad M \equiv N - 1\,. \tag{3.13}$$

We now are in a position to estimate when τ cannot be considered to be small anymore and the approximation first breaks down.

In (3.1) set $j = M$ and choose k so that $\theta_k = -\theta_M$. We see that by keeping only the $n = 0$ term in the sum we neglected, for example, the following potentially large term,

$$\frac{1}{2\theta_M - 2\pi}\,. \tag{3.14}$$

This is the point where ignoring periodicity becomes unacceptable. At $N \gg 1$ our small-τ approximation breaks down for

$$2\sqrt{\tau}\left(1 - \frac{1.856}{(2N)^{2/3}}\right) \approx \pi\,. \tag{3.15}$$

JHEP05(2009)107

In conclusion, the small-τ approximation holds for

$$\sqrt{\tau} \ll \frac{\pi}{2} \tag{3.16}$$

if $N \gg 1$, but extends further if N is not too large. Since we know that at infinite N there is a transition at $\tau = 4$, we see that the small-τ approximation cannot take us all the way to the critical point for $N \gg 1$.

The most important conclusion is that the expansion in scale for small loops yields a spectrum restricted to a finite arc centered at zero angle and that the boundaries of the arc approach their infinite-N limits by a leading term of order $N^{-2/3}$. This exponent is a well-known property of the Gaussian ensemble of Hermitian matrices, and is connected to universal functions constructed out of the Airy function. The Airy function is in turn familiar from WKB wave functions at linear turning points. The power of 3 that appears in the exponent of its integral representation is related to the denominator 3 in the power of N we just saw.

As the scale of the loop grows, the boundaries of the arc expand, until they meet each other at $\theta = \pm\pi$, at which point the small-scale expansion breaks down and the exponent changes.

3.2 $\theta_j(\tau)$ for large τ

3.2.1 The eigenvalues at $\tau = \infty$

The eigenvalues expand away from zero until they stop at $\tau = \infty$, at which point they are equally spaced and contained in the interval $(-\pi, \pi)$. Throughout the expansion they maintain the sum rule

$$\sum_{j=0}^{N-1} \theta_j(\tau) = 0\,. \tag{3.17}$$

This determines their asymptotic limits,

$$\theta_j(\tau = \infty) = \frac{2\pi}{N}\left(j - \frac{N-1}{2}\right) \equiv \Theta_j\,, \qquad j = 0, \ldots, N-1\,. \tag{3.18}$$

We now prove that the above configuration is an equilibrium point in the sense that the τ-derivatives of the $\theta_j(\tau)$ vanish for $\theta_j = \Theta_j$, $j = 0, \ldots, N-1$. Since

$$\dot{\theta}_j = -\frac{i}{2N} \sum_{k \neq j} \frac{1 + e^{i(\theta_j - \theta_k)}}{1 - e^{i(\theta_j - \theta_k)}} \tag{3.19}$$

we need to show that for each $j = 0, \ldots, N-1$

$$\sum_{k \neq j} \frac{1 + e^{i(\Theta_j - \Theta_k)}}{1 - e^{i(\Theta_j - \Theta_k)}} = 0\,. \tag{3.20}$$

Let us denote by q the N-roots of unity. A sum over q runs over these N complex numbers. We need to show that

$$A = \sum_{q \neq 1} \frac{1+q}{1-q} = 0\,. \tag{3.21}$$

This would then imply (3.20). The above equation already implies that the l.h.s. of (3.20) is independent of j. Dividing by q the numerator and denominator of the summand and noticing that the restriction $q \neq 1$ is identical to the restriction $1/q \neq 1$ for the N-roots of unity q, we get $A = -A = 0$.

However, we shall soon need to evaluate other sums over q, and for these a more general procedure is needed. This procedure, when applied to the present trivial case, goes as follows. Start from

$$A = \lim_{x\to 1^-} \left[\sum_q \left(\frac{1+xq}{1-xq} \right) - \frac{1+x}{1-x} \right] . \tag{3.22}$$

Next,

$$\begin{aligned} A &= \lim_{x\to 1^-} \left[-N + 2 \sum_{n\geq 0} x^n \sum_q q^n - \frac{1+x}{1-x} \right] = \lim_{x\to 1^-} \left[-N + 2N \sum_{k\geq 0} x^{kN} - \frac{1+x}{1-x} \right] \\ &= \lim_{x\to 1^-} \left[-N + \frac{2N}{1-x^N} - \frac{1+x}{1-x} \right] = \lim_{\epsilon\to 0^+} \left[-N + \left(\frac{2}{\epsilon} + N - 1 \right) - \frac{2-\epsilon}{\epsilon} \right] = 0 . \end{aligned} \tag{3.23}$$

This again proves (3.20). Above, we observed that $\sum_q q^n$ will be zero if n is not a multiple of N, and N otherwise. We need $x < 1$ to perform the expansion in a geometric series, but at the end we can take $x \to 1$. Similar techniques work for all other sums over q we shall need.

3.2.2 Linearization of the large-τ equation

We now expand around the infinite-τ solution, to see how it is approached. From the exact formula for $\langle \det(z - W) \rangle$ in [4], we expect the approach to be exponentially rapid, with decay constants given by the Casimirs of the antisymmetric representations labeled by l, where $l = 1, \ldots, N-1$. This is $N-1$ nonzero values, not N. The missing value corresponds to a uniform τ-independent shift in all $\theta_j(\tau)$, which is a symmetry of the differential equation. This symmetry would produce a zero mode in the linearized equation, but the mode is eliminated by the sum rule (3.17), which depends also on the initial condition.

To linearize we set

$$\theta_j(\tau) = \Theta_j + \delta\theta_j(\tau) \tag{3.24}$$

and expand the equation of motion to linear order in $\delta\theta_j$. Unlike the initial condition, the set $\{\Theta_j\}$ provides a nondegenerate configuration around which it is straightforward to expand. We find

$$\delta\dot{\theta}_j = -\frac{1}{4N} \sum_{k=0}^{N-1} A_{jk} \delta\theta_k \tag{3.25}$$

with the matrix A given by

$$A_{jk} = \begin{cases} -\frac{1}{\sin^2 \frac{\Theta_j - \Theta_k}{2}} & \text{for } k \neq j , \\ \sum_{k\neq j} \frac{1}{\sin^2 \frac{\Theta_j - \Theta_k}{2}} & \text{for } k = j . \end{cases} \tag{3.26}$$

We need the eigenvalues and eigenvectors of this matrix. Note first that A_{jj} does not depend on j and is given by

$$A_{jj} = 4 \sum_{q \neq 1} \frac{1}{(1-q)(1-q^{-1})} \,. \tag{3.27}$$

The sum over q can be performed as before leading to

$$A_{jj} = \frac{N^2-1}{3} \,. \tag{3.28}$$

Hence, the matrix A has entries A_{ij} which only depend on $(i-j)$ mod N. Therefore, A has N eigenvectors $\phi^{(l)}$ with components $\phi^{(l)}_k$, $k, l = 0, \ldots, N-1$, given by

$$\phi^{(l)}_k = \frac{1}{\sqrt{N}} e^{-i\frac{\pi l(N-1)}{N}} e^{i\frac{2\pi l}{N}k} \,. \tag{3.29}$$

The phases have been chosen for later convenience. To evaluate the action of A on an eigenvector $\phi^{(l)}$, we need to perform sums of the type

$$\xi^{(l)} = -4 \sum_{q \neq 1} \frac{q^l}{(1-q)(1-q^{-1})} \,. \tag{3.30}$$

The sum over q is performed as before, and one gets

$$\xi^{(l)} + \frac{N^2-1}{3} = 2l(N-l) \,. \tag{3.31}$$

The r.h.s. is the eigenvalue of A corresponding to the l-th eigenvector $\phi^{(l)}$. $l = 0$ corresponds to the zero mode which does not contribute to the $\delta\theta_j$, so we are left with $N-1$ contributing modes, labeled by $l = 1, \ldots, N-1$. As expected, the eigenvalues of A come out proportional to the quadratic Casimirs in the l-fold antisymmetric representation, given by [14]

$$C_2(l) = \frac{N+1}{N} l(N-l) \,. \tag{3.32}$$

The equations of motion (2.15) have the values of the Casimirs encoded in them.

Thus we have found that

$$\delta\theta_k(\tau) = \sum_{l=1}^{N-1} C_l \phi^{(l)}_k e^{-\frac{\tau}{2N} l(N-l)} \,. \tag{3.33}$$

It remains to determine the coefficients C_l. Since the leading asymptotic terms at large τ correspond to $l = 1$ and $l = N-1$, we only need C_1.

3.2.3 Constraints on the coefficients

The coefficients C_l are restricted by two quite trivial exact general properties, which imply for the $\delta\theta_k(\tau)$ that

$$\delta\theta_k(\tau) = \delta\theta^*_k(\tau) \,, \qquad\qquad \delta\theta_k(\tau) = -\delta\theta_{N-k-1}(\tau) \,. \tag{3.34}$$

JHEP05(2009)107

These constraints lead to

$$\delta\theta_k(\tau) = \sum_{l=1}^{N-1} \rho_l \sin\left[\frac{2\pi l}{N}(k+1/2)\right] e^{-\frac{\tau}{2N}l(N-l)} \tag{3.35}$$

with real ρ_l and

$$\rho_l = \rho_{N-l}\,. \tag{3.36}$$

Every term in the sum representing $\delta\theta_k(\tau)$ is invariant under $l \to N-l$.

3.2.4 Leading asymptotic behavior

Note first that we have

$$\langle \mathrm{Tr}\, W\rangle = \sum_{k=0}^{N-1} e^{i\theta_k}\,, \tag{3.37}$$

which is the term proportional to z^{N-1} in the expansion of (2.9) in z.

For the leading asymptotic behavior of the $\theta_k(\tau)$ we only need ρ_1. We can obtain ρ_1 from the exact result

$$\frac{1}{N}\langle \mathrm{Tr}\, W\rangle = e^{-\frac{\tau}{2N}(N-1)}\,. \tag{3.38}$$

Actually, we only need this result at leading order as $\tau \to \infty$. To linear order in $\delta\theta_k$, and keeping only the terms with $l=0$ and $l=N-1$ in (3.35), we have

$$\frac{1}{N}\langle \mathrm{Tr}\, W\rangle = -\frac{2i}{N}\rho_1 \sum_{k=0}^{N-1} e^{\frac{2\pi i}{N}(k+1/2)} \sin\left[\frac{2\pi}{N}(k+1/2)\right] e^{-\frac{\tau}{2N}(N-1)}\,. \tag{3.39}$$

Performing the trivial sum over k we get

$$\rho_1 = 1\,. \tag{3.40}$$

Hence, as $\tau \to \infty$

$$\delta\theta_k(\tau) \sim 2\sin\left[\frac{2\pi}{N}(k+1/2)\right] e^{-\frac{\tau}{2N}(N-1)} \tag{3.41}$$

or, more completely,

$$\theta_k(\tau) \sim \frac{\pi}{N}(2k+1-N) + 2\sin\left[\frac{2\pi}{N}(k+1/2)\right] e^{-\frac{\tau}{2N}(N-1)}\,. \tag{3.42}$$

Equivalently, we can write

$$\theta_k(\tau) \sim \Theta_k - 2e^{-\frac{\tau}{2N}(N-1)}\sin(\Theta_k)\,. \tag{3.43}$$

For Θ_k negative the correction is positive and for Θ_k positive the correction is negative. This shows that, as expected, for increasing τ each eigenvalue is distancing itself from the origin for all k. The correction is largest for eigenvalues in the middle of the upper and lower half of the circle — the eigenvalues here are the last to settle into their infinite-τ destinations.

3.3 Extremal $\theta_j(\tau)$ for $\tau \sim 4$ and large N

3.3.1 Universal zeros

In terms of the variable y from [4], the zeros corresponding to the angles $\theta_j(\tau)$ mod 2π are given by

$$\hat{q}_N\left(i(\theta_j(\tau)-\pi),\tau\right)=0 \tag{3.44}$$

with

$$\hat{q}_N(y,\tau)=\int_{-\infty}^{\infty} dx\, e^{-\frac{N}{2\tau}(y-x)^2} e^{N\log(2\cosh(x/2))}\,. \tag{3.45}$$

The universal form of $\hat{q}_N(y,\tau)$ for large N, $y\sim 0$, and $\tau\sim 4$ is obtained by replacing the $\log(2\cosh(x/2))$ above by its expansion truncated at order x^4,

$$\log\left(\cosh\frac{x}{2}\right)=\frac{x^2}{8}-\frac{x^4}{192}\,. \tag{3.46}$$

At $\tau=4$, we have

$$\hat{q}_N(y,4)=\int_{-\infty}^{\infty} dx\, e^{-\frac{N}{8}(x-y)^2} e^{N\log(2\cosh(x/2))}\,. \tag{3.47}$$

The "universal zeros" y_*^j are defined by

$$\int_{-\infty}^{\infty} dx\, e^{-\frac{N}{192}(x^4-48xy_*^j)}=0\,. \tag{3.48}$$

3.3.2 Universal numerical values

Universal zeros have been investigated in [15]. Define

$$\frac{Nx^4}{192}=\mu u^4\,,\qquad\qquad \frac{Nxy_*^j}{4}=4i\mu u\,. \tag{3.49}$$

Then

$$y_*^k=\pm i\frac{4\sqrt{2}}{3}\left(\frac{3\mu_k}{N}\right)^{3/4}\,, \tag{3.50}$$

where the μ_k, $k=1,2,\ldots$ are the zeros of

$$F(\mu)=\int du\, e^{\mu(4iu-u^4)}\,. \tag{3.51}$$

From table 1 of [15], we have $\mu_1=0.8221, \mu_2=2.0227,\ldots$ Various other results concerning the μ_k can be found in [15]. For the extremal positive zero at $\tau=4$ we need to look at y_*^1,

$$y_*^1\approx i\frac{3.7}{N^{3/4}}\,. \tag{3.52}$$

This gives, for large N, that the zero $z_j(\tau_c)$ that is closest to -1 with $\mathrm{Im}\, z_j>0$ is

$$z_M\approx e^{i(\pi-3.7N^{-3/4})}\,. \tag{3.53}$$

JHEP05(2009)107

4 Asymptotic expansion of $\rho_N^{\mathrm{sym}}(\theta, T)$

The aim of this section is to construct an asymptotic expansion of $\rho_N^{\mathrm{sym}}(\theta, T)$ in powers of $1/N$. To this end we perform a saddle-point analysis of the integral in (2.26), from which $\rho_N^{\mathrm{sym}}(\theta, T)$ can be obtained via (2.22) and (2.23). It is sufficient to study only $\psi_+^{(N)}(z, T)$ because $\psi_-^{(N)}(z, T)$ can be obtained from (2.21).

4.1 Saddle-point analysis

For $|z| = 1$ the integrand of (2.26) has singularities on the real-u axis. We therefore set $z = e^{\epsilon + i\theta}$, where $\epsilon > 0$ ensures that $|z| > 1$ but will later be taken to zero. The integrand of (2.26) can be written as $\exp(-Nf(u))$ with

$$f(u) = \frac{u^2}{2T} + \log\left(ze^{-i\frac{u}{2}} - e^{i\frac{u}{2}}\right). \tag{4.1}$$

We now look for saddle points of the integrand in the complex-u plane, which we label by $\bar{u} = iTU(\theta, T)$, where $\mathrm{U}(\theta, T) = U_r(\theta, T) + iU_i(\theta, T)$ is a complex-valued function of θ and T. The saddle-point equation turns out to be

$$e^{-TU(\theta,T)}\frac{\mathrm{U}(\theta, T) + 1/2}{\mathrm{U}(\theta, T) - 1/2} = e^{\epsilon + i\theta}. \tag{4.2}$$

For $\epsilon = 0$, this is equation (5.49) in [8] and is related to the inviscid complex Burgers equation via equation (5.44) there. In the present notation, the latter equation has the form

$$\frac{\partial U}{\partial T} + iU\frac{\partial U}{\partial \theta} = 0. \tag{4.3}$$

Taking the absolute value of (4.2) leads to the equation

$$U_i^2 = U_r \coth(TU_r + \epsilon) - U_r^2 - \frac{1}{4}. \tag{4.4}$$

For $\epsilon = 0$, this equation has been investigated previously in [8]. However, here we keep $\epsilon > 0$ for the time being. The singularities of the integrand of (2.26) then all have $U_r < 0$. Equation (4.4) describes one or more curves in the complex-U plane on which the saddle points have to lie (for a given value of θ, the saddles are isolated points on these curves). In figure 2 we show typical examples for these curves for $T < 4$, $T = 4$, and $T > 4$, where ϵ has been chosen sufficiently close to zero. (The closed contours always enclose the points $U = 1/2$ or $U = -1/2$. For $T > 4$ and larger ϵ, the closed contour in the left half-plane would be missing, but right now we are not concerned with this since we are only interested in the limit $\epsilon \to 0^+$.) Analyzing (4.2) numerically we find, for all values of T, that for a given value of θ there is always one (and only one) saddle point on the closed contour in the right half-plane, i.e., with $U_r > 0$. Note that we are showing the complex-U plane, in which the original integration contour corresponds to the imaginary axis. The integration contour can be smoothly deformed to go through the (single) saddle point in the right half-plane along a path of steepest descent. No singularities are crossed since they all have

JHEP05(2009)107

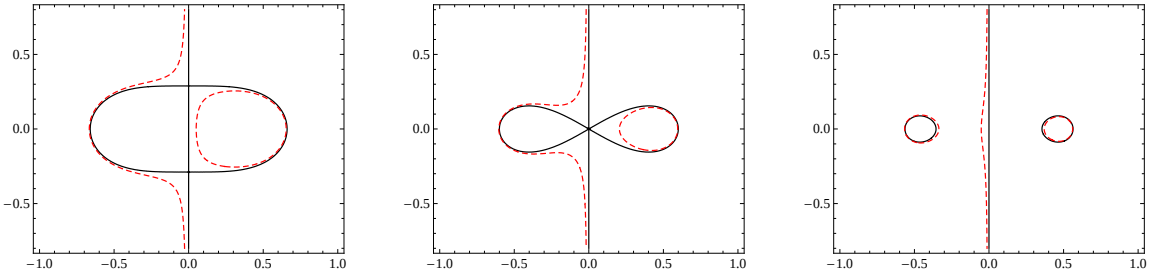

Figure 2. Examples of the contours in the complex-U plane described by equation (4.4) for $T = 3$ (left), $T = 4$ (middle), and $T = 5$ (right). The red dashed curves are for small $\epsilon > 0$, while the solid black curves are for $\epsilon = 0$. For our saddle-point analysis we keep $\epsilon > 0$.

$U_r < 0$. There are also saddle points on the contour(s) in the left half-plane (in fact, there are infinitely many on the open contour), but these need not be considered.

Once the integration contour has been deformed to go through the saddle point, we can safely take the limit $\epsilon \to 0^+$. Parametrizing the contour in the vicinity of the saddle point by $u = \bar{u} + xe^{i\beta}$, where x is the new integration variable corresponding to the fluctuations around the saddle and β is the angle which the path of steepest descent makes with the real-u axis, $\psi_+^{(N)}(e^{i\theta}, T)$ is given, up to exponentially small corrections in N, by

$$\psi_+^{(N)}(e^{i\theta}, T) = \frac{1}{2^N}\sqrt{\frac{N}{2\pi T}}\, e^{\frac{NT}{8} - i\frac{N\theta}{2} + i\beta} \int_{-\infty}^{\infty} dx\, e^{-Ng(x)}\,, \tag{4.5}$$

$$g(x) = \frac{1}{2T}\big(xe^{i\beta} + iTU(\theta, T)\big)^2 + \log\sinh\frac{i\theta - ixe^{i\beta} + TU(\theta, T)}{2}\,. \tag{4.6}$$

We can now expand $g(x)$ in x. The linear order vanishes by construction. The second order gives a Gaussian integral over x, resulting in

$$\psi_+^{(N)}(e^{i\theta}, T) \approx e^{\frac{NT}{8} + \frac{NTU^2(\theta,T)}{2}} \frac{\big[e^{-i\theta}(1/4 - U^2(\theta, T))\big]^{N/2}}{\sqrt{1 - T(1/4 - U^2(\theta, T))}}\,. \tag{4.7}$$

Note that the factor $e^{-i\theta}$ cannot be pulled out of the term in square brackets because periodicity in θ would be lost.

There is a potential complication. In principle, $g''(0)$ and therefore the denominator in (4.7) could be zero, which would mean that the integral over x cannot be performed in Gaussian approximation. For $T > 4$, it is straightforward to show that $g''(0)$ is never zero. For $T \leq 4$, one can use (4.2) to show that $g''(0) = 0$ only for the saddle points corresponding to the two angles $\theta = \pm\theta_c(T)$ at which $\rho_\infty(\theta, T)$ becomes zero (see section 2.5). This means that for $|\theta| = \theta_c(T)$ the asymptotic expansion in $1/N$ diverges, and that it converges ever more slowly as $|\theta| \to \theta_c$ from below.

Note that for $T < 4$ and $\theta_c(T) \leq |\theta| \leq \pi$ the function $\rho^{\text{sym}}(\theta, T)$ is exponentially suppressed in N. The study of the large-N asymptotic behavior in this region requires more work.

JHEP05(2009)107

4.2 Leading-order result

Equation (4.7) is the leading order in the $1/N$ expansion of $\psi_+^{(N)}(e^{i\theta},T)$. We now show that it leads to $\rho_N^{\rm sym}(\theta,T)\to\rho_\infty(\theta,T)$ as $N\to\infty$. We first write (4.7) in the form

$$\frac{1}{N}\log\psi_+^{(N)}(e^{i\theta},T)=\frac{T}{8}-f(\bar u)+\mathcal{O}(1/N)\,. \tag{4.8}$$

Note that in this order we do not need the denominator in (4.7), which corresponds to $f''(\bar u)$ (or $g''(0)$). Via (2.22) and using $\bar u=iTU$ this leads to

$$\phi_+^{(N)}(z,T)=i\left(\frac12-\frac{z}{z-e^{-TU}}\right)+\mathcal{O}(1/N)=-iU+\mathcal{O}(1/N)\,, \tag{4.9}$$

where in the last step we have used the saddle-point equation (4.2). Equation (2.23) then gives

$$\lim_{N\to\infty}\rho_N^{\rm sym}(\theta,T)=2\,\mathrm{Re}\,\mathrm{U}(\theta,T)\,, \tag{4.10}$$

which equals $\rho_\infty(\theta,T)$ of DO [1, 17] since $\mathrm{U}(\theta,T)$ satisfies (4.2) (which leads to (5.51) below with $\lambda=U-1/2$ and $v=1/z$).

4.3 $1/N$ correction to $\rho_\infty(\theta,T)$

Higher-order terms in the $1/N$ expansion of $\psi_+^{(N)}(e^{i\theta},T)$ can be obtained in the standard way by considering higher powers of x in the expansion of $g(x)$, resulting in integrals of the type $\int_{-\infty}^{\infty}dx\,x^{2n}e^{-g''(0)x^2/2}$ with $n\in\mathbb{N}$. However, if we are only interested in the $1/N$ correction to $\rho_\infty(\theta,T)$ the result (4.7) is already sufficient ($1/N$ corrections to this result would give $1/N^2$ corrections to $\rho_\infty(\theta,T)$). Therefore we now write

$$\frac{1}{N}\log\psi_+^{(N)}(e^{i\theta},T)=\frac{T}{8}-f(\bar u)-\frac{1}{2N}\log[Tf''(\bar u)]+\mathcal{O}(1/N^2)\,, \tag{4.11}$$

which leads to

$$\phi_+^{(N)}(z,T)=-iU\left(1+\frac{1}{N}\frac{T(1/4-U^2)}{[1-T(1/4-U^2)]^2}\right)+\mathcal{O}(1/N^2) \tag{4.12}$$

and thus to

$$\rho_N^{\rm sym}(\theta,T)=2\,\mathrm{Re}\left[U\left(1+\frac{1}{N}\frac{T(1/4-U^2)}{[1-T(1/4-U^2)]^2}\right)\right]+\mathcal{O}(1/N^2)\,. \tag{4.13}$$

Note that for $T\le 4$ and $|\theta|\to\theta_c(T)$ (from below) the denominator of the $1/N$ term approaches zero, which corresponds to the complication discussed in section 4.1. Note also that for $T\le 4$ and $|\theta|>\theta_c$ the saddle point $\mathrm{U}(\theta,T)$ is purely imaginary so that both the leading order and the $1/N$ term are zero. This confirms that the above saddle-point analysis is not the right tool to compute finite-N effects in this region.

In figure 3 we show examples for the $1/N$ corrections to $\rho_\infty(\theta,T)$ for $N=10$ and $T=2$ and 5.

JHEP05(2009)107

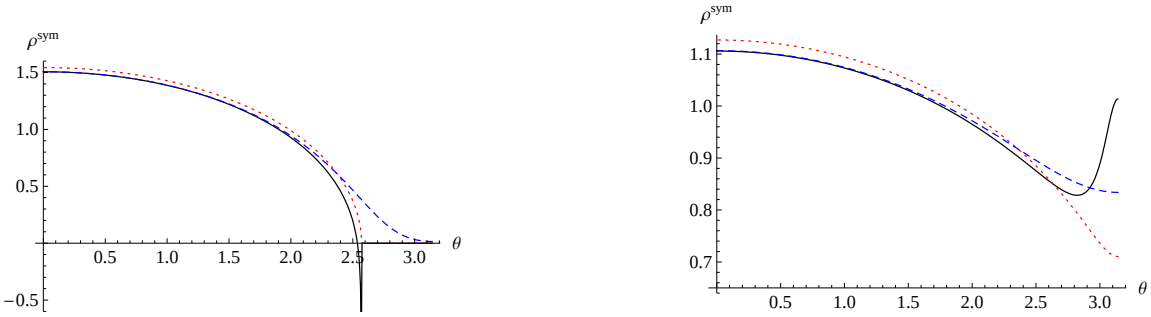

Figure 3. Examples for the $1/N$ corrections to $\rho_\infty(\theta,T)$ for $N=10$, $T=2$ (left), and $T=5$ (right). Shown are the exact result for $\rho_N^{\rm sym}(\theta,T)$ (blue dashed curve), the infinite-N result $\rho_\infty(\theta,T)$ (red dotted curve), and the asymptotic expansion of $\rho_N^{\rm sym}(\theta,T)$ up to order $\mathcal{O}(1/N)$ from (4.13) (black solid curve). We observe that the asymptotic expansion converges rapidly for small $|\theta|$ and more slowly for larger $|\theta|$.

5 The true eigenvalue density at finite N

We now proceed to derive exact formulas for the eigenvalue density $\rho_N^{\rm true}(\theta,t)$.

5.1 Character expansion

To compute (2.30) we consider the ratio of determinants

$$R(u,v,W)\equiv\frac{\det(1+uW)}{\det(1-vW)} \tag{5.1}$$

with $|v|<1$ and expand it in SU(N) characters using [5]

$$\det(1+uW)=\sum_{p=0}^{N}u^p\chi_p^A(W)\,,\qquad\qquad \det(1-vW)=\sum_{q=0}^{\infty}v^q\chi_q^S(W)\,, \tag{5.2}$$

where $\chi_p^A(W)$ ($\chi_q^S(W)$) denotes the character of W in a totally antisymmetric (symmetric) representation whose Young diagram consists of a single column (row) with p (q) boxes. The trivial representation corresponds to $p=0$ ($q=0$), and for SU(N) the antisymmetric representation with $p=N$ boxes is equivalent to the trivial one because of $\chi_N^A(W)=\det W=1$. This yields

$$R(u,v,W)=\sum_{p=0}^{N}\sum_{q=0}^{\infty}u^pv^q\chi_p^A(W)\chi_q^S(W)\,. \tag{5.3}$$

The task now is to decompose the tensor product $p^A\otimes q^S$ into irreducible representations. In general, $p^A\otimes q^S$ consists of tensors with $p+q$ indices, where the first p are antisymmetrized and the last q are symmetrized. To decompose into irreducible representations we take one index from the first p and one from the last q and either symmetrize or antisymmetrize this pair. There are no more symmetrization operations we can perform. Thus, $p^A\otimes q^S$ decomposes into two irreducible representations, except in boundary cases when it is already

JHEP05(2009)107

irreducible. The boundary cases are at $q = 0$ or $p = 0$ or $p = N$. Away from the boundary cases $p^A \otimes q^S$ decomposes into two irreducible representations identified by Young diagrams with the top row consisting of h boxes and a left column of v boxes and nothing else:

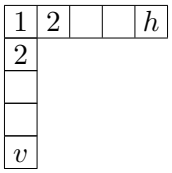

(5.4)

One either has $h = q$ and $v = p+1$ or $h = q+1$ and $v = p$. (Do not confuse the v here with the argument of R.) The first case corresponds to an antisymmetrized pair and the second to a symmetrized pair. For later convenience we shall label the "hook" diagram in (5.4) by $(v-1, h-1)$, with the understanding that $v = 0$ or $h = 0$ gives the trivial representation. We thus have

$$p^A \otimes q^S = (p, q-1) \oplus (p-1, q) \tag{5.5}$$

and for the boundary cases

$$p^A \otimes 0 = (p-1, 0)\,, \quad 0 \otimes q^S = (0, q-1)\,, \quad N^A \otimes q^S = (N-1, q) = (0, q-1)\,. \tag{5.6}$$

Taking into account these boundary cases and suppressing the SU(N) matrix argument W, we obtain

$$R(u,v) = 1 + \sum_{p=0}^{N-1}\sum_{q=1}^{\infty} u^p v^q \chi_{(p,q-1)} + \sum_{p=1}^{N}\sum_{q=0}^{\infty} u^p v^q \chi_{(p-1,q)}\,. \tag{5.7}$$

The case $p = 0$, $q = 0$ is excluded from the sums. Every other boundary case appears in exactly one of the two sums above. Every nontrivial pair has one of the two irreducible representations in exactly one of the sums. Now change summation indices $q \to q+1$ in the first sum and $p \to p+1$ in the second to obtain

$$R(u,v) = 1 + (u+v)\sum_{p=0}^{N-1}\sum_{q=0}^{\infty} u^p v^q \chi_{(p,q)}\,. \tag{5.8}$$

This makes it explicit that $R = 1$ at $u = -v$.

A consequence is the character expansion of $\operatorname{Tr} W^k$ for all k. Since

$$R(-v+\epsilon, v) = 1 - \frac{N\epsilon}{v} + \frac{\epsilon}{v}\operatorname{Tr}\frac{1}{1-vW} + \mathcal{O}(\epsilon^2)\,, \tag{5.9}$$

we have

$$\operatorname{Tr}\frac{1}{1-vW} = N + v\sum_{(p,q)}(-1)^p v^{p+q}\chi_{(p,q)}(W)\,, \tag{5.10}$$

where the limits on the double sum are given in (5.8). Hence, taking $k > 0$,

$$\operatorname{Tr} W^k = \sum_{\substack{(p,q)\\ p+q=k-1}} (-1)^p \chi_{(p,q)}(W)\,. \tag{5.11}$$

Obviously, $\operatorname{Tr} 1 = N$ and $\operatorname{Tr} W^{-k} = (\operatorname{Tr} W^k)^*$.

5.2 Performing the average

The average over W with weight (2.4) produces, using character orthogonality,

$$\langle \chi_{(p,q)}(W) \rangle = d(p,q) e^{-\frac{t}{2N} C(p,q)} , \tag{5.12}$$

where $C(p,q)$ is the value of the quadratic Casimir operator in (p,q), given by [14]

$$C(p,q) = (p+q+1)\left(N - \frac{p+q+1}{N} + q - p \right) \tag{5.13}$$

and the dimension of the irreducible representation labeled by (p,q) is

$$d(p,q) = d^A(p) d^S(q) \frac{(N-p)(N+q)}{N} \frac{1}{p+q+1} \tag{5.14}$$

with

$$d^A(p) = \binom{N}{p} , \qquad d^S(q) = \binom{N+q-1}{q} . \tag{5.15}$$

5.3 Basic combinatorial identities

The expansions of one determinant or one inverse determinant factor (i.e., setting $W = 1$ and $u = \xi$, $v = 0$ or $u = 0$, $v = \eta$ in (5.8)) provide the identities

$$\Sigma^A(\xi) \equiv \sum_{p=0}^{N-1} \xi^p d^A(p)(N-p) = N(1+\xi)^{N-1} , \tag{5.16a}$$

$$\Sigma^S(\eta) \equiv \sum_{q=0}^{\infty} \eta^q d^S(q)(N+q) = \frac{N}{(1-\eta)^{N+1}} , \tag{5.16b}$$

with $|\eta| < 1$. These will be needed to carry out the summations over p and q later.

5.4 Factorizing the sums over p and q for the average resolvent at zero area

Set $u = -v + \epsilon$. Up to corrections of order ϵ^2 we have

$$R(-v+\epsilon, v, W) = 1 + \epsilon \sum_{p=0}^{N-1} \sum_{q=0}^{\infty} (-1)^p v^{p+q} \chi_{(p,q)}(W) = 1 - \epsilon \operatorname{Tr} \frac{1}{v - W^\dagger} . \tag{5.17}$$

This leads to

$$\bar{R}(v) \equiv \left\langle \operatorname{Tr} \frac{1}{v - W^\dagger} \right\rangle = - \sum_{p=0}^{N-1} \sum_{q=0}^{\infty} (-1)^p v^{p+q} e^{-\frac{t}{2N} C(p,q)} d(p,q) , \tag{5.18}$$

where $t = \lambda \mathcal{A}$. Note that the sum can be extended to $p = N$ because of the factor $N - p$ in $d(p,q)$. Using (2.30) and (2.31), we obtain

$$\rho^{\text{true}}(\theta, t) = 1 - \frac{2}{N} \lim_{\epsilon \to 0^+} \operatorname{Re}[v \bar{R}(v)] , \qquad v = e^{-\epsilon + i\theta} . \tag{5.19}$$

Note that there is no need for the limiting procedure $\epsilon \to 0^+$ in (5.19) if we are using the double sum in (5.18) for $\bar{R}(v)$, which is well-defined for $|v| = 1$.

We now introduce an integral to get rid of the denominator in (5.14) and obtain

$$\bar{R}(v) = -\int_0^1 \frac{d\rho}{N} \sum_{p=0}^{N} \sum_{q=0}^{\infty} \left[(-1)^p v^p \rho^p d^A(p)(N-p)\right] \left[v^q \rho^q d^S(q)(N+q)\right] \times e^{-\frac{t}{2N}(p+q+1)(N-\frac{p+q+1}{N}+q-p)} . \tag{5.20}$$

This achieves factorization of the sums over p and q at $t = 0$. The sum in each factor can be performed using (5.16).

5.5 Integral representation at any area

The t-dependent weight factor is the exponent of a bilinear form in p and q. By a Hubbard-Stratonovich transformation the dependence of the exponent on p and q can be made linear, and then the sums over p and q are factorized for every t and can again be done exactly using (5.16).

Define the complex symmetric matrix B_N by

$$B_N = \begin{pmatrix} 1+\frac{1}{N} & \frac{i}{N} \\ \frac{i}{N} & 1-\frac{1}{N} \end{pmatrix} . \tag{5.21}$$

B_N has only one eigenvalue (equal to one) and is nondiagonalizable. We have $\det B_N = 1$ and

$$B_N^{-1} = \begin{pmatrix} 1-\frac{1}{N} & -\frac{i}{N} \\ -\frac{i}{N} & 1+\frac{1}{N} \end{pmatrix} . \tag{5.22}$$

The quadratic Casimir form can be written with the help of B_N:

$$C(p,q) = \begin{pmatrix} ip \\ q \end{pmatrix}^T B_N \begin{pmatrix} ip \\ q \end{pmatrix} + N\left(1-\frac{1}{N^2}\right) + N\left(1+\frac{1}{N}-\frac{2}{N^2}\right) q + N\left(1-\frac{1}{N}-\frac{2}{N^2}\right) p . \tag{5.23}$$

Hence

$$e^{-\frac{t}{2N}C(p,q)} = \frac{N}{t}\, e^{-\frac{t}{2}\left(1-\frac{1}{N^2}\right)} \int_{-\infty}^{\infty}\int_{-\infty}^{\infty} \frac{dxdy}{2\pi} \exp\left[-\frac{N}{2t}\begin{pmatrix} x & y \end{pmatrix} B_N^{-1} \begin{pmatrix} x \\ y \end{pmatrix}\right] \times e^{-px+iqy} \exp\left\{-\frac{t}{2}\left[\left(1+\frac{1}{N}-\frac{2}{N^2}\right) q + \left(1-\frac{1}{N}-\frac{2}{N^2}\right) p\right]\right\} . \tag{5.24}$$

Using (5.16) we now perform the sums over p and q,

$$\bar{R}(v) = -\frac{N^2}{t}\, e^{-\frac{t}{2}\left(1-\frac{1}{N^2}\right)} \times \int_{-\infty}^{\infty}\int_{-\infty}^{\infty} \frac{dxdy}{2\pi} \exp\left[-\frac{N}{2t}[(1-1/N)x^2 + (1+1/N)y^2 - 2ixy/N]\right] \times \int_0^1 d\rho \, \frac{\left[1-v\rho e^{-x-(t/2)(1-1/N-2/N^2)}\right]^{N-1}}{\left[1-v\rho e^{iy-(t/2)(1+1/N-2/N^2)}\right]^{N+1}} . \tag{5.25}$$

Note that because of $|v| < 1$ the denominator in the last line is never zero. The integral over ρ can be done exactly, if one wishes, resulting in

$$\bar{R}(v) = \frac{N}{t}\, e^{-\frac{t}{2}(1-\frac{1}{N^2})} \int_{-\infty}^{\infty}\int_{-\infty}^{\infty} \frac{dxdy}{2\pi} \left\{ \left[\frac{1 - v\, e^{-x-(t/2)(1-1/N-2/N^2)}}{1 - v\, e^{iy-(t/2)(1+1/N-2/N^2)}} \right]^N - 1 \right\}$$
$$\times \frac{e^{-\frac{N}{2t}[(1-1/N)x^2+(1+1/N)y^2-2ixy/N]}}{v\left[e^{-x-(t/2)(1-1/N-2/N^2)} - e^{iy-(t/2)(1+1/N-2/N^2)}\right]}\,. \tag{5.26}$$

The above formula was derived for $|v| < 1$; this is enough for finding $\rho_N^{\rm true}(\theta)$ via (5.19). Using symmetries of $\langle R(u,v,W)\rangle$ one can immediately write down also results for $|v| > 1$.

5.6 Making sense of negative integer N

Conforming to previous observations (see [10] and references therein), we extend our result to negative integer N. This may be of relevance to $1/2N$ playing the role of the viscosity term in Burgers' equation [4, 5] and also to approximate equations in [16].

We first restate the result derived earlier,

$$\bar{R}(u,v,N) \equiv \langle R(u,v,W)\rangle$$
$$= 1 + \frac{u+v}{N} \sum_{p=0}^{N-1}\sum_{q=0}^{\infty} \frac{1}{p+q+1} u^p v^q e^{-\frac{\lambda_A}{2}\hat{C}(p,q,N)} M^A(p,N) M^S(q,N)\,, \tag{5.27}$$

where

$$\hat{C}(p,q,N) = \frac{C(p,q,N)}{N} = (p+q+1)\left(1 - \frac{p+q+1}{N^2} + \frac{q-p}{N}\right)\,, \tag{5.28a}$$
$$M^A(p,N) = \frac{(N-p)(N-p+1)\cdots N}{(p+1)!}(p+1)\,, \tag{5.28b}$$
$$M^S(q,N) = \frac{(N+q)(N+q-1)\cdots N}{(1+q)!}(q+1)\,. \tag{5.28c}$$

In equations (5.28) p and q still are nonnegative integers, but N is allowed to be an integer of arbitrary sign (with $N = 0$ excluded).

Note that for $p \geq N$, $M^A(p,N) = 0$. Hence, still keeping $N > 0$, we can remove one of the restrictions on the range of p in the sum in equation (5.27),

$$\bar{R}(u,v,N) = 1 + \frac{u+v}{N} \sum_{p,q=0}^{\infty} \frac{1}{p+q+1} u^p v^q e^{-\frac{\lambda_A}{2}\hat{C}(p,q,N)} M^A(p,N) M^S(q,N)\,. \tag{5.29}$$

Observe

$$\hat{C}(p,q,-N) = \hat{C}(q,p,N)\,, \tag{5.30a}$$
$$M^A(p,-N) = (-1)^{p+1} M^S(p,N)\,, \tag{5.30b}$$
$$M^S(q,-N) = (-1)^{q+1} M^A(q,N)\,. \tag{5.30c}$$

The entire dependence on N in (5.29) is explicit, and the function $\bar{R}(u,v,N)$ remains well-defined for $N<0$, so long as the fixed parameter $\lambda\mathcal{A}$ is positive. With $N>0$ this leads to

$$\bar{R}(u,v,N)=1+\frac{-u-v}{-N}\sum_{p,q=0}^{\infty}\frac{(-u)^p(-v)^q}{p+q+1}M^S(p,-N)M^A(q,-N)e^{-\frac{\lambda\mathcal{A}}{2}\hat{C}(q,p,-N)}\,. \tag{5.31}$$

Interchanging the dummy summation labels p and q we get

$$\bar{R}(u,v,N)=\bar{R}(-v,-u,-N)\,. \tag{5.32}$$

Writing

$$\bar{R}(u,v,N)=1+\frac{u+v}{N}\Omega(u,v,N) \tag{5.33}$$

produces

$$\Omega(u,v,N)=\Omega(-v,-u,-N)\,. \tag{5.34}$$

Now set $u=-v$. $\Omega(-v,v,N)$ is finite for $\lambda\mathcal{A}>0$. We have

$$\Omega(-v,v,N)=\Omega(-v,v,-N)\,. \tag{5.35}$$

$\Omega(-v,v,N)$ determines $\rho_N^{\rm true}(\theta,t)$ via (5.19) because of $\Omega(-v,v,N)=N\bar{R}(v)$, i.e.,

$$\rho_N^{\rm true}(\theta,t)=1+\frac{2}{N^2}\lim_{\epsilon\to 0^+}\mathrm{Re}\left[v\,\Omega(-v,v,N)\right],\qquad v=e^{-\epsilon+i\theta}\,. \tag{5.36}$$

At this point we realize that we have defined $\rho_N^{\rm true}(\theta,t)$ for negative integer N, too:

$$\rho_{-N}^{\rm true}(\theta,t)=1+\frac{2}{N}\lim_{\epsilon\to 0^+}\mathrm{Re}\left[v\,\Omega(-v,v,-N)\right]=\rho_N^{\rm true}(\theta,t)\,, \tag{5.37}$$

where in the last step we have observed (5.35).

5.7 Large-N asymptotics

If one could expand $\rho_N^{\rm true}(\theta,t)$ in N around $N=0$, only even powers of N would enter. However, all one can do is an asymptotic expansion in $1/N$, and then odd powers will appear. Essentially, the asymptotic expansion is not in $1/N$ but rather in $1/|N|$. For example, for small loops there is an arc centered at $\pm\pi$ where the infinite-N eigenvalue density has a gap, and there at finite N one has exponential suppression of the form $\exp(-|N|\kappa)$, $\kappa>0$ — it makes no sense to drop the absolute value on N in the exponent. As another example, consider a sub-leading term that goes like $\cos(N\theta)/|N|$. The oscillatory behavior of $\rho_N^{\rm true}(\theta,t)$ comes from a contribution of this type.

We now turn to the integral representation to take the first steps in a $1/N$ expansion of $\rho_N^{\rm true}(\theta,t)$. Shifting integration variables $x\to x+(t/2)\left(1/N+2/N^2\right)$ and $y\to y-i(t/2)\left(1/N-2/N^2\right)$ in (5.25), we obtain

$$\bar{R}(v)=-\frac{N^2}{t}e^{-\frac{t}{2}}\iint_{-\infty}^{\infty}\frac{dxdy}{2\pi}\int_0^1 d\rho\,e^{-\frac{N}{2t}(x^2+y^2)+\frac{1}{2t}(x+iy)^2-\frac{1}{2}(x-iy)}\frac{\left[1-v\rho e^{-x-t/2}\right]^{N-1}}{\left[1-v\rho e^{iy-t/2}\right]^{N+1}}\,. \tag{5.38}$$

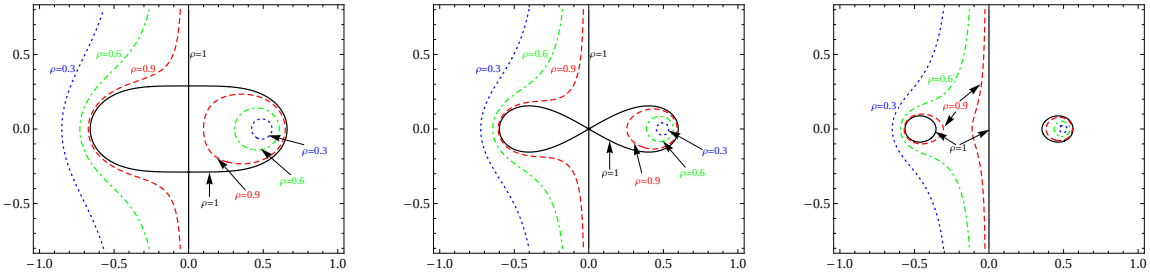

Figure 4. Contours of solutions of equation (5.41) in the complex-U plane at $t = 3$ (left), $t = 4$ (middle), and $t = 5$ (right) for $\rho = 1$ (black, solid), $\rho = 0.9$ (red, dashed), $\rho = 0.6$ (green, dot-dashed), and $\rho = 0.3$ (blue, dotted). In the figures (but not in the analysis) we have taken $|v| = 1$ for simplicity.

Since this integral representation was derived for $|v| < 1$, we set $v = e^{i\theta-\epsilon}$ with $|\theta| \leq \pi$, $\epsilon > 0$, and take the limit $\epsilon \to 0$ at the end. We write (5.38) as

$$\bar{R}(v) = -\frac{N^2}{t} e^{-\frac{t}{2}} \iint_{-\infty}^{\infty} \frac{dxdy}{2\pi} \int_0^1 d\rho\, e^{-\frac{N}{2t}\left(x^2+y^2\right)+\frac{1}{2t}(x+iy)^2-\frac{1}{2}(x-iy)} \times e^{(N-1)\log\left(1-v\rho e^{-x-t/2}\right)-(N+1)\log\left(1-v\rho e^{iy-t/2}\right)}\,. \tag{5.39}$$

At large N, the integrals over x and y decouple at leading order and can be done independently by saddle-point approximations. Let us start with the integral over y since it is conceptually simpler. The y-dependent coefficient of the term in the exponent in equation (5.39) that is proportional to $-N$ is

$$\bar{f}(y) = \frac{1}{2t}y^2 + \log\left[1 - v\rho e^{iy-\frac{t}{2}}\right]\,. \tag{5.40}$$

Substituting $y = u - it/2 = it(U - 1/2)$ (with $u = itU$ in analogy to section 4) results in exactly the same integrand that was already considered in section 4, with the replacements $T \to t$ and $z \to 1/v\rho$ (with $|v\rho| < 1$) and with an integration over u that is now along the line from $-\infty + it/2$ to $+\infty + it/2$. Since there are no singularities between this line and the real-u axis we can change the integration path to be along the real-u (or imaginary-U) axis. Now everything goes through as in section 4. The saddle-point equation reads

$$e^{-tU}\frac{U + 1/2}{U - 1/2} = \frac{1}{v\rho}\,, \tag{5.41}$$

which is equivalent to (4.2). In figure 4 we show the contours in the complex-U plane on which the solutions of the saddle-point equation have to lie. (For sufficiently small ρ we now encounter the case mentioned in section 4.1 where for $t > 4$ the closed contour in the left half-plane is missing.) The relevant saddle point, which we denote by $y_0(\theta, t, \rho)$, is again on the closed contour in the right half-plane. For decreasing ρ this contour contracts, but this makes no difference to our analysis. The result for the y-integral is given by an expression similar to (4.7).

JHEP05(2009)107

We now turn to the integral over x. The x-dependent coefficient of the term in the exponent in equation (5.39) that is proportional to $-N$ is

$$\tilde{f}(x) = \frac{1}{2t}x^2 - \log\left[1 - v\rho e^{-x-t/2}\right] = -\bar{f}(ix)\,. \tag{5.42}$$

Substituting $x = -iu - t/2 = t(U - 1/2)$ (with $u = itU$) again leads to the integral considered in section 4 and the saddle-point equation (5.41), except that the integration is now along the real-U axis. The positions of the saddle points of the x-integral are obtained by rotating the saddles of the y-integral by $-\pi/2$ in the complex-U plane, i.e., $x_s = -iy_s$. At a saddle point we have

$$\tilde{f}''(x_s) = \frac{1}{t} + \frac{x_s}{t}\left(1 + \frac{x_s}{t}\right) = \bar{f}''(y_s)\,, \tag{5.43}$$

and therefore the directions of steepest descent through a saddle y_s and the corresponding saddle $x_s = -iy_s$ are identical (no rotation). By analyzing the directions along which the phase of the integrand is constant, we find that the integration contour can always be deformed to go through the (single) saddle-point in the right half-plane in the direction of steepest descent. Depending on the parameters ρ, v, and t, there is either one or no additional saddle point on the contour(s) in the left half-plane through which we can also go in the direction of steepest descent. If there is such an additional saddle point, we find that its contribution to the integral is always exponentially suppressed in N compared to the saddle point in the right half-plane and can therefore be dropped from the saddle-point analysis. In addition, there are infinitely many more saddle points on the open contour in the left half-plane. However, we cannot deform the integration path to go through these points in the direction of steepest descent and therefore do not need to include them. An example for the location of the saddle points and the deformation of the integration path is given in figure 5. To summarize, the x-integral can be approximated by the contribution of the single saddle point in the right half-plane, which again leads to an expression similar to (4.7).

Combining the saddle-point approximations for the integrals over x and y, we find that, up to exponentially small corrections in N, the integral in equation (5.39) is given by

$$\bar{R}(v) = -\frac{N^2}{t}e^{-t/2}\int_0^1 d\rho\,\frac{1}{2\pi}\left(\frac{2\pi}{N\tilde{f}''(x_0)}\right)\frac{1}{(1 - v\rho e^{-x_0-t/2})^2}\,e^{-x_0}\,, \tag{5.44}$$

where $x_0 = x_0(\theta, t, \rho)$ is the dominating saddle point of the x-integral. x_0 is a solution of the saddle-point equation obtained by differentiating $\tilde{f}(x)$, which can be written as

$$v\rho e^{-x_0-t/2} = \frac{x_0}{x_0 + t} \tag{5.45}$$

and leads to

$$\left(1 - v\rho e^{-x_0-\frac{t}{2}}\right)^2 = \left(\frac{t}{t + x_0}\right)^2\,. \tag{5.46}$$

With (5.43) we obtain

$$\tilde{f}''(x_0)\left(1 - v\rho e^{-x_0-\frac{t}{2}}\right)^2 = \frac{t + x_0\,(t + x_0)}{(t + x_0)^2} \tag{5.47}$$

JHEP05(2009)107

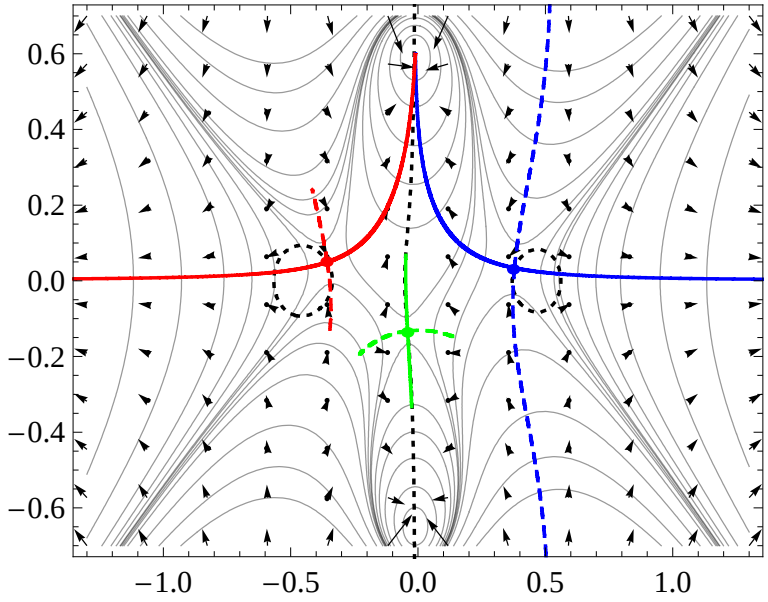

Figure 5. Example for the location of the saddle points and the deformation of the integration path in the complex-U plane for $t = 5$ and $\rho = 0.95$. The dashed black curves (two closed, one open) are the curves on which all saddle points have to lie, cf. (4.4). In this example $\theta = 3.0$. On each of the closed curves there is one saddle point (red dot and blue dot), and on the open curve there are infinitely many saddle points, but only one of them in the region shown in the plot (green dot). The thin solid lines are lines of constant $\mathrm{Re}\,\tilde{f}(x)$ and $\mathrm{Re}\,\bar{f}(y)$. The arrows point in the direction of increasing $\mathrm{Re}\,\tilde{f}(x)$ or decreasing $\mathrm{Re}\,\bar{f}(y)$. The dashed blue curve is the integration path for the y-integral along the direction of steepest descent. The solid red-blue curve is the integration path for the x-integral along the direction of steepest descent.

and

$$\bar{R}(v) = -\frac{N}{t} e^{-\frac{t}{2}} \int_0^1 d\rho \, \frac{(t+x_0)^2}{t+x_0\,(t+x_0)} \, e^{-x_0} \,. \tag{5.48}$$

Differentiating equation (5.45) with respect to ρ leads to

$$\frac{\partial x_0}{\partial \rho} = \frac{1}{\rho} \frac{x_0\,(t+x_0)}{t+x_0\,(t+x_0)} = v e^{-x_0 - t/2} \frac{(t+x_0)^2}{t+x_0\,(t+x_0)} \,, \tag{5.49}$$

which yields

$$\bar{R}(v) = -\frac{N}{tv} \int_0^1 d\rho \, \frac{\partial x_0}{\partial \rho} = -\frac{N}{tv} \left[x_0(\theta, t, \rho = 1) - x_0(\theta, t, \rho = 0) \right] \,. \tag{5.50}$$

We know from (5.45) that $x_0(\theta, t, \rho = 0) = 0$. If we parametrize $x_0(\theta, t, \rho = 1) = \lambda(\theta, t) t$, where $\lambda(\theta, t)$ has to solve

$$\lambda = \frac{1}{\frac{1}{v} e^{t(\lambda + 1/2)} - 1} \,, \tag{5.51}$$

and take the limit $\epsilon \to 0^+$, we end up with

$$\bar{R}(v) = -\frac{N \lambda(\theta, t)}{v} \,, \qquad v = e^{i\theta} \,. \tag{5.52}$$

JHEP05(2009)107

Here we need to keep in mind that we have to pick the solution of equation (5.51) which corresponds to the dominating saddle point x_0 of the x-integral for $|v\rho| < 1$.

Using (5.19) we obtain

$$\lim_{N\to\infty} \rho_N^{\text{true}}(\theta,t) = 1 + 2\,\text{Re}\,\lambda(\theta,t)\,, \tag{5.53}$$

which is equal to $\rho_\infty(\theta,t)$ [1, 17]. Keeping higher orders in the saddle-point approximation (as explained in section 4.3), we can compute the asymptotic expansion of $\rho_N^{\text{true}}(\theta,t)$ in powers of $1/N$.

5.8 A partial differential equation for the average of the ratio of characteristic polynomials at different arguments

In the expression for $\Omega(u,v,N)$ that follows from (5.29) a derivative with respect to t will bring down the Casimir factor from the exponent. Writing

$$u = -e^{X+Y}\,, \qquad v = e^{X-Y}\,, \qquad f_N(X,Y,t) = \Omega(u,v,N)|_{t=\lambda\mathcal{A}} \tag{5.54}$$

we can reconstruct the Casimir by derivatives with respect to X and Y. All that comes in is the bilinear structure of the Casimir. We obtain

$$\frac{\partial f_N}{\partial t} = \frac{1}{2}\left[\frac{1}{N^2}\left(\frac{\partial}{\partial X}+1\right)^2 - \left(1-\frac{1}{N}\frac{\partial}{\partial Y}\right)\left(\frac{\partial}{\partial X}+1\right)\right] f_N\,. \tag{5.55}$$

One can simplify the equation by $f_N \to g_N = e^{X-NY} f_N$,

$$\frac{\partial g_N}{\partial t} = \frac{1}{2}\left(\frac{1}{N^2}\frac{\partial^2}{\partial X^2} + \frac{1}{N}\frac{\partial^2}{\partial Y \partial X}\right) g_N\,. \tag{5.56}$$

Rescaling $X \to NX = Z$ removes all explicit dependence on N in the equation. The equation is linear, so we are free to rescale g_N by any power of N we find convenient. We define

$$G_N(Z,Y,t) \equiv \frac{1}{N} g_N(Z/N,Y,t) \tag{5.57}$$

and now have

$$\frac{\partial G_N}{\partial t} = \frac{1}{2}\left(\frac{\partial^2}{\partial Z^2} + \frac{\partial^2}{\partial Y \partial Z}\right) G_N\,. \tag{5.58}$$

The N-dependence of G_N will then come in only through the initial condition at $t = 0$. We proceed to find the initial condition. Similarly to (5.16) the combinatorial factors $M^{A,S}$ have the following generating functions:

$$\sum_{p=0}^{\infty} M^A(p,N) A^p = N(1+A)^{N-1}\,, \tag{5.59a}$$

$$\sum_{q=0}^{\infty} M^S(q,N) S^q = \frac{N}{(1-S)^{N+1}}\,. \tag{5.59b}$$

These identities go beyond (5.16) in that they hold also for negative integer N. Using

$$\frac{1}{p+q+1} = \int_0^1 d\rho\, \rho^{p+q} \tag{5.60}$$

and the fact that at $t = 0$ we have

$$\Omega(u, v, N)|_{t=0} = \sum_{p,q=0}^{\infty} \frac{u^p v^q}{p+q+1} M^A(p, N) M^S(q, N) \tag{5.61}$$

we obtain

$$\Omega(u, v, N)|_{t=0} = N^2 \int_0^1 d\rho\, \frac{(1+\rho u)^{N-1}}{(1-\rho v)^{N+1}}\,. \tag{5.62}$$

Observing that

$$\frac{\partial}{\partial r} \frac{(1+rA)^N}{(1+rB)^N} = N(A-B) \frac{(1+rA)^{N-1}}{(1+rB)^{N+1}} \tag{5.63}$$

we derive

$$\Omega(u, v, N)|_{t=0} = \frac{N}{u+v} \left[\left(\frac{1+u}{1-v} \right)^N - 1 \right]. \tag{5.64}$$

From this we now find the initial condition associated with equation (5.58),

$$G_N(Z, Y, t=0) = -\frac{e^{-NY}}{e^Y - e^{-Y}} \left[\left(\frac{1 - e^{\frac{Z}{N}+Y}}{1 - e^{\frac{Z}{N}-Y}} \right)^N - 1 \right]. \tag{5.65}$$

The partial differential equation (5.58) and the associated initial condition (5.65) admit arbitrary N, no longer restricted to integers, although for noninteger N periodicity in θ is lost. However, periodicity in θ was assumed when the relation between ρ_N^{true} and Ω was derived.

One can again check whether there is a symmetry under $N \to -N$. The partial differential equation is linear and invariant under

$$Z \to -Z\,, \qquad Y \to -Y\,, \qquad N \to -N\,. \tag{5.66}$$

The initial condition switches sign under this transformation. Hence,

$$G_N(Z, Y, t) = -G_{-N}(-Z, -Y, t)\,. \tag{5.67}$$

For noninteger N there is some subtlety in defining the cuts in the initial condition so that the above holds.

By Fourier/Laplace transforms one can derive integral representations, embedding the initial condition at $t \to 0$. To get to the density $\rho_N^{\text{true}}(\theta, t)$ via (5.19) and $\bar{R}(v) = \Omega(-v, v, N)/N$, one needs to set $u = -v$, which corresponds to $Y = 0$ at fixed $Z/N = -\epsilon + i\theta$, i.e.,

$$\rho_N^{\text{true}}(\theta, t) = 1 + \frac{2}{N} \lim_{\epsilon \to 0^+} \text{Re}\; G_N(N(-\epsilon + i\theta), 0, t)\,. \tag{5.68}$$

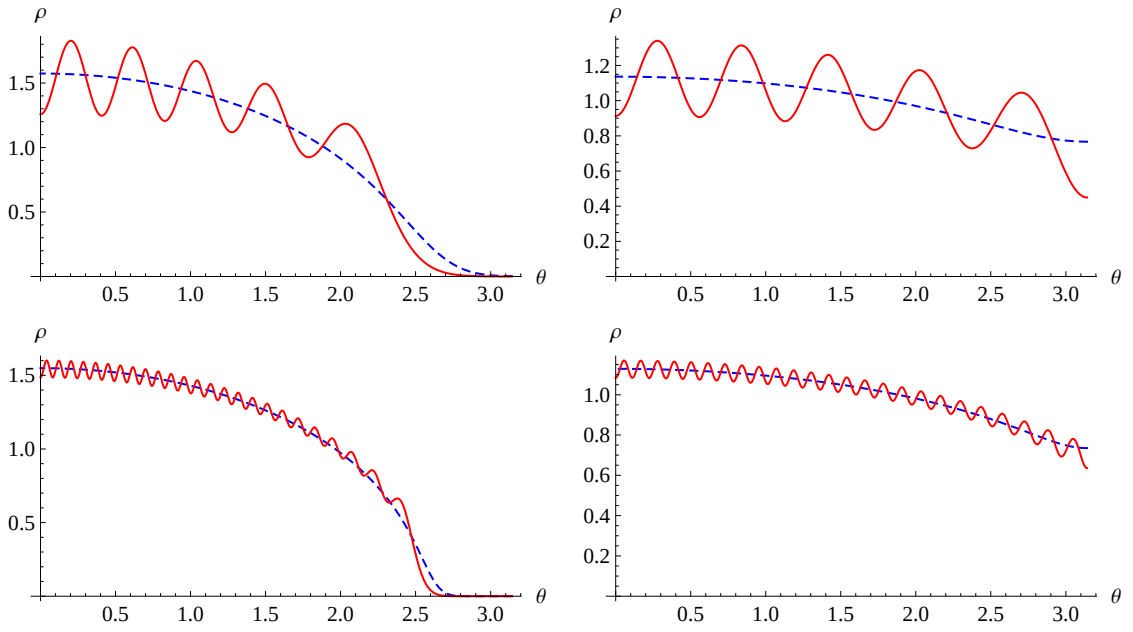

Figure 6. Plots of the densities $\rho_N^{\rm true}(\theta,t)$ (red, solid) and $\rho_N^{\rm sym}(\theta,T)$ (blue, dashed) for $t=2$ (left) and $t=5$ (right), $N=10$ (top), and $N=50$ (bottom).

At $t>0$ the limit should be smooth, but at $t=0$ one needs to generate a δ-function singularity in $\rho_N^{\rm true}(\theta,t)$ at $\theta=0$ mod 2π. We first need the $Y\to 0$ limit of (5.65), which is

$$G_N(Z,Y=0,t=0)=\frac{Ne^{Z/N}}{1-e^{Z/N}}=\frac{Ne^{-\epsilon+i\theta}}{1-e^{-\epsilon+i\theta}}\,. \tag{5.69}$$

Expanding the denominator in a geometric series and using (5.68) yields

$$\rho_N^{\rm true}(\theta,t=0)=1+e^{i\theta}\sum_{k=0}^{\infty}e^{ik\theta}+e^{-i\theta}\sum_{k=0}^{\infty}e^{-ik\theta}=\sum_{k=-\infty}^{\infty}e^{ik\theta}=2\pi\delta_{2\pi}(\theta) \tag{5.70}$$

as expected. $\rho_N^{\rm true}(\theta,t=0)$ is independent of N.

6 Comparison of the three eigenvalue densities

6.1 $\rho_N^{\rm true}(\theta,t)$ and $\rho_N^{\rm sym}(\theta,T)$

If we want to compare $\rho_N^{\rm true}(\theta,t)$ and $\rho_N^{\rm sym}(\theta,T)$ we have to take into account the $1/N$ difference between t and T, see equation (2.3). At fixed N and t, we have to compare $\rho_N^{\rm true}(\theta,t)$ and $\rho_N^{\rm sym}(\theta,T=t(1-1/N))$. The densities $\rho_N^{\rm true}$ and $\rho_N^{\rm sym}$ can be obtained numerically by evaluating the sums in equation (5.18) and equation (2.25), respectively.

Figure 6 shows plots of $\rho_N^{\rm true}(\theta,t)=\rho_N^{\rm true}(-\theta,t)$ and $\rho_N^{\rm sym}(\theta,T)=\rho_N^{\rm sym}(-\theta,T)$ for $t=2$, $t=5$, $N=10$, and $N=50$ in the interval $0\le\theta\le\pi$. As stated in section 2.5, $\rho_N^{\rm sym}(\theta,T)$ decreases monotonically in that interval. The true eigenvalue density $\rho_N^{\rm true}(\theta,t)$ has N peaks (in the complete interval $[-\pi,\pi]$) and oscillates around the nonoscillatory function $\rho_N^{\rm sym}(\theta,T)$.

JHEP05(2009)107

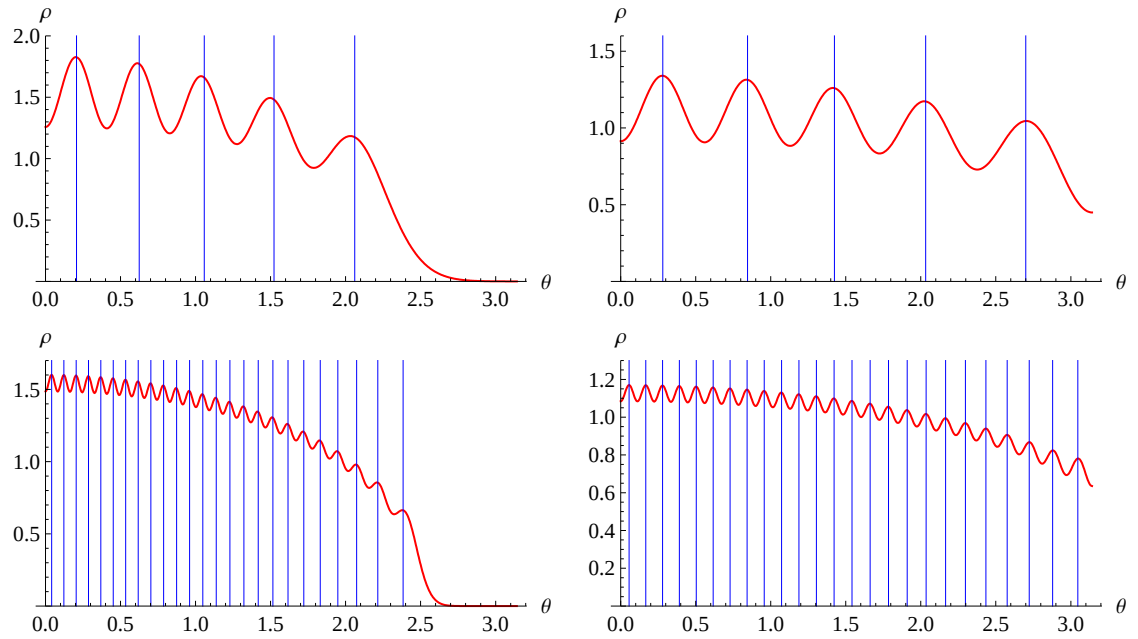

Figure 7. Plots of the density $\rho_N^{\text{true}}(\theta, t)$ (oscillatory red curve) together with the positions of the zeros of $\langle \det(e^{i\theta} - W) \rangle$ (vertical blue lines) for $t = 2$ (left) and $t = 5$ (right), $N = 10$ (top), and $N = 50$ (bottom).

6.2 $\rho_N^{\text{true}}(\theta, t)$ and $\rho_N^{\text{asym}}(\theta, \tau)$

The density $\rho_N^{\text{asym}}(\theta, \tau)$ is given by a sum of N δ-functions, located at the zeros of the average characteristic polynomial, see section 2.4. Figure 7 shows that the locations of these zeros are close to the positions of the N peaks of $\rho_N^{\text{true}}(\theta, t)$. Here we again have to take into account the $1/N$ difference in the definitions of t and τ. For fixed N and t, the peaks of $\rho_N^{\text{true}}(\theta, t)$ have to be compared to the zeros of $\langle \det(e^{i\theta} - W) \rangle$ at $\tau = t(1 + 1/N)$.

Computing the positions of the peaks and valleys of ρ^{true} and the corresponding zeros of the average characteristic polynomial for large N shows that the difference in position between a peak and its matching zero vanishes faster than the difference in position between that peak and the next valley. This means that

$$\gamma = \left| \frac{\theta^{(\text{peak})} - \theta^{(\text{matching zero})}}{\theta^{(\text{peak})} - \theta^{(\text{next valley})}} \right| \tag{6.1}$$

scales like

$$\gamma \propto N^{-\mu} \quad \text{with} \quad \mu > 0\,. \tag{6.2}$$

It turns out that the value of the exponent μ depends on t and may be different in different parts of the spectrum, but it is always positive (for large N).

In the bulk of the spectrum, the difference between peak and neighboring valley scales like N^{-1}, whereas the difference between peak and matching zero scales like N^{-2} for all t. This results in $\mu_{\text{bulk}} = 1$. Figure 8 shows a plot of $\log \gamma$, computed for the peak closest to $\theta = 0$, as a function of $\log N$ for $t = 5$. The line fitted through the data points has a

JHEP05(2009)107

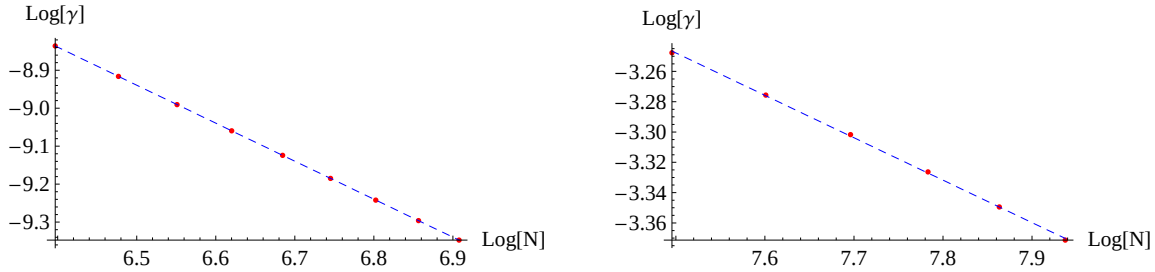

Figure 8. Plots of $\log\gamma$ for the peak closest to $\theta = 0$ at $t = 5$ (left) and for the peak closest to $\theta = \pi$ at $\tau = 4$ (right). Data points (red) are shown together with the fitted line (blue, dashed).

slope of $-1 + O(10^{-3})$. (The reason for choosing θ close to 0 is that stable fit results can be obtained for lower values of N.)

For $t > 4$, the infinite-N limit of the eigenvalue density, $\rho_\infty(\theta, t)$, has no gap. In this case the scaling behavior does not change as one goes to higher $|\theta|$, but it is necessary to go to large values of N to get stable fit results for μ when $|\theta|$ is close to π. (E.g., for $t = 5$ a fit at $N \approx 1000$ results in $\mu \approx 1.04$ for the extremal peak.)

At the transition point the situation is different. From equation (3.53) we know that the difference between the position of the extremal zero (the zero closest to π) and π scales like $N^{-0.75}$ for $\tau = 4$. Between $N = 1800$ and $N = 2800$, the difference between the extremal zero and its critical-τ approximation scales roughly like $N^{-1.25}$, the difference between that zero and the extremal peak position scales like $N^{-1.11}$, and the difference between the positions of the peak and the next valley (the valley that is closer to $\theta = 0$) scales like $N^{-0.83}$. This results in $\mu_{\text{critical}} \approx 0.28$. The plot of $\log\gamma$ for that case (see figure 8) indicates that the value of μ_{critical} might slightly increase as one goes to even higher values of N (which requires more computation time).

For $t < 4$ there is a gap in the spectrum. In this case, the exponent μ also has different values at the edge and the bulk of the spectrum, but the variation is not as large as it is at the critical point. E.g., for $t = 3$ a fit between $N = 1000$ and $N = 1500$ results in $\mu \approx 0.64$ for the extremal peak. For small $|\theta|$ we again find $\mu = \mu_{\text{bulk}} = 1$. Naturally, we expect the exact values of the various exponents of N that enter to be rational numbers with denominators 3 or 4 or 12 (see section 3.1.4).

7 The bigger picture

For definiteness consider four-dimensional (Euclidean) pure SU(N) Yang-Mills theory. Focus on the string tension and think about a lattice formulation using a single-plaquette action $S = \sum_p s(U_p)$, where p denotes a plaquette. For a fixed N one can choose s such that no phase transitions occur for all bare real couplings g_0. One can define a "string tension", for example, by using a Creutz ratio,

$$\sigma_{\text{Creutz}}(L, g_0) = -\log \frac{\langle \operatorname{Tr} W(L, L+1)\rangle \langle \operatorname{Tr} W(L+1, L)\rangle}{\langle \operatorname{Tr} W(L, L)\rangle \langle \operatorname{Tr} W(L+1, L+1)\rangle}\,, \tag{7.1}$$

JHEP05(2009)107

where $W(L_1, L_2)$ is the Wilson loop matrix for a rectangular loop measuring $L_1 \times L_2$ in lattice units.

$\sigma_{\text{Creutz}}(L, g_0)$ can be expanded around $g_0 \to 0$ and $g_0 \to \infty$. The regimes of validity of these two expansions are disjoint; in between there is a crossover regime and we can bridge it only by numerical calculation. There are extra complications around $g_0 = \infty$. Rectangular loops of the type usually used have a "roughening" nonanalyticity in g_0. This nonanalyticity is a lattice artifact. It can be avoided by choosing loops at generic angles with lattice planes. Then, the definition of σ_{Creutz} needs to be extended. All this will increase the complexity of the strong-coupling expansion. At the end, only a physical crossover separating the ranges of the weak- and strong-coupling expansion remains. We have no nonnumerical calculational method to bridge it. To get the continuum string tension in units of the perturbative scale Λ we need to take the continuum limit, a correlated limit in which $g_0 \to 0$ and the overall lattice scale of the loop goes to infinity. This correlated limit preserves the crossover.

The idea we are pursuing is to improve the above scheme in two respects. First, since we wish to set up a calculation in the continuum we forget about the lattice. Instead of thinking about σ_{Creutz} we consider some other observable, for definiteness the extremal eigenvalue θ_M of a Wilson loop of size λ.

For this to make sense, we need to be able to define θ_M in renormalized continuum field theory. We hope that this can be done by first constructing a renormalized polynomial in z corresponding to $\langle \det(z - W) \rangle$ and taking the roots of it to define θ_M. While we have some idea how a calculation for small loops might proceed, for large loops we need something beyond ordinary field theory. Here we assume that an effective string model will describe $\langle \det(z - W) \rangle$. This model will have a dimensional parameter, the string tension, and will be a good description for very large loops, with corrections parametrized by more parameters becoming more and more important as the loop shrinks.

To relate the string tension to Λ, the dimensional parameter entering the perturbation theory for small loops, one needs to join the two regimes over the crossover. Here is the point that the simplification of large N enters: At infinite N the crossover for z_M collapses into a point, and we have a phase transition. We postulate that we know that the transition is universal and that we know it is in the same universality class as the DO transition.

Therefore, for $N \gg 1$, the dependence of z_M on intermediate scales, i.e., scales in the vicinity of the critical scale, is known up to a few constants. This is the ingredient that was missing in the lattice scenario described above. It is now possible to imagine calculating to some order at short, intermediate, and long scales, and sew together the three scale ranges. Requiring smooth matches could produce a number for the string tension in units of the perturbative scale Λ.

There are many variations possible. z_M is only one possible example of a potentially useful variable. z_M depends on the dilation of a fixed-shaped Wilson loop, measured by a dimensionless variable λ. As a function of λ, z_M will trace out a trajectory from $\theta = 0$ at $\lambda = 0$ (one could replace this by a $0 < \lambda_0 \ll 1$) to $\theta = \pi(1 - 1/2N)$ at $\lambda = \infty$. For small λ, the perturbative scale Λ enters the calculations, and for large λ the string tension enters. The two regimes are joined by the crossover. To parametrize the crossover one has to work out the details of the two-dimensional case.

In two-dimensional YM renormalization is trivial, perturbation theory is well-defined, and there even exists an exact string description [9]. We need to gain control over the crossover at large N, and then we can try to build a prototype of the calculation we envisage. We also need to learn enough to open the possibility of finding other interesting observables than θ_M. This is where the present paper fits in.

Acknowledgments

We acknowledge support by BayEFG (RL), by the DOE under grant number DE-FG02-01ER41165 at Rutgers University (HN), and by DFG and JSPS (TW). HN also notes with regret that his research has for a long time been deliberately obstructed by his high energy colleagues at Rutgers. HN thanks G. Dunne for bringing ref. [10] to his attention. TW thanks the Theoretical Hadron Physics Group at Tokyo University for their hospitality.

References

[1] B. Durhuus and P. Olesen, *The spectral density for two-dimensional continuum QCD*, *Nucl. Phys.* **B 184** (1981) 461 [SPIRES].

[2] R. Narayanan and H. Neuberger, *Universality of large-N phase transitions in Wilson loop operators in two and three dimensions*, *JHEP* **12** (2007) 066 [arXiv:0711.4551] [SPIRES].

[3] R. Narayanan, H. Neuberger and E. Vicari, *A large-N phase transition in the continuum two dimensional* SU(N) × SU(N) *principal chiral model*, *JHEP* **04** (2008) 094 [arXiv:0803.3833] [SPIRES].

[4] H. Neuberger, *Burgers' equation in* 2D SU(N) *YM*, *Phys. Lett.* **B 666** (2008) 106 [arXiv:0806.0149] [SPIRES].

[5] H. Neuberger, *Complex Burgers' equation in* 2D SU(N) *YM*, *Phys. Lett.* **B 670** (2008) 235 [arXiv:0809.1238] [SPIRES].

[6] J.-P. Blaizot and M.A. Nowak, *Large-N_c confinement and turbulence*, *Phys. Rev. Lett.* **101** (2008) 102001 [arXiv:0801.1859] [SPIRES].

[7] E. Gudowska-Nowak, R.A. Janik, J. Jurkiewicz and M.A. Nowak, *Infinite products of large random matrices and matrix-valued diffusion*, *Nucl. Phys.* **B 670** (2003) 479 [math-ph/0304032] [SPIRES].

[8] R. Lohmayer, H. Neuberger and T. Wettig, *Possible large-N transitions for complex Wilson loop matrices*, *JHEP* **11** (2008) 053 [arXiv:0810.1058] [SPIRES].

[9] D.J. Gross and W. Taylor, *Two-dimensional QCD is a string theory*, *Nucl. Phys.* **B 400** (1993) 181 [hep-th/9301068] [SPIRES].

[10] G.V. Dunne, *Negative dimensional groups in quantum physics*, *J. Phys.* **A 22** (1989) 1719 [SPIRES].

[11] M.L. Mehta, *Random matrices*, second edition, Academic Press, San Diego CA U.S.A. (1991).

[12] H.S. Wilf, *Mathematics for the physical sciences*, Dover (1978).

[13] G. Szegö, *Orthogonal polynomials*, American Mathematical Society, Providence RI U.S.A. (1991).

JHEP05(2009)107

[14] A.M. Perelomov and V.M. Popov, *Casimir operators for the unitary group*, *JETP Letters* **1** (1965) 160.

[15] D. Senouf, *Asymptotic and numerical approximations of the zeros of Fourier integrals*, *SIAM J. Math. Anal.* **27** (1996) 1102.

[16] J.-P. Blaizot and M.A. Nowak, *Universal shocks in random matrix theory*, arXiv:0902.2223 [SPIRES].

[17] R.A. Janik and W. Wieczorek, *Multiplying unitary random matrices — universality and spectral properties*, *J. Phys. A: Math. Gen.* **37** (2004) 6521.

JHEP05(2009)107